Check for updates

Received: 24 May 2023 | Revised: 12 July 2023 | Accepted: 2 October 2023

DOI: 10.1002/jbt.23554

RESEARCH ARTICLE

WILEY

New palladium complexes with *N*-heterocyclic carbene and morpholine ligands: Synthesis, characterization, crystal structure, molecular docking, and biological activities

Ayten Behçet[1] | Parham Taslimi[2] | Betül Şen[3] | Tuğba Taskın-Tok[4,5] | Aydın Aktaş[6] | Yetkin Gök[1] | Muhittin Aygün[3] | İlhami Gülçin[7]

[1]Department of Chemistry, Faculty of Science and Arts, Inonu University, Malatya, Türkiye

[2]Department of Biotechnology, Faculty of Science, Bartin University, Bartin, Türkiye

[3]Department of Physics, Faculty of Science, Dokuz Eylül University, Buca, Türkiye

[4]Department of Chemistry, Faculty of Arts and Sciences, Gaziantep University, Gaziantep, Türkiye

[5]Institute of Health Sciences, Gaziantep University, Gaziantep, Türkiye

[6]Vocational School of Health Service, Inonu University, Malatya, Türkiye

[7]Department of Chemistry, Faculty of Science, Atatürk University, Erzurum, Türkiye

Correspondence
Parham Taslimi, Department of Biotechnology, Faculty of Science, Bartin University, Bartin, Türkiye.
Email: parham_taslimi_un@yahoo.com

Funding information
Bartin Üniversitesi, Grant/Award Number: 2020-FEN-B-005; Dokuz Eylül Üniversitesi, Grant/Award Number: 2010.KB.FEN.13

Abstract

This work includes the synthesis of a new series of palladium-based complexes containing both morpholine and *N*-heterocyclic carbene (NHC) ligands. The new complexes were characterized using NMR (^{1}H and ^{13}C), FTIR spectroscopic, and elemental analysis techniques. The crystal structure of complex **1b** was obtained by utilizing the single-crystal X-ray diffraction method. X-ray studies show that the coordination environment of palladium atom is completed by the carbene carbon atom of the NHC ligand, the nitrogen atom of the morpholine ring, and a pair of bromide ligand, resulting in the formation of slightly distorted square planar geometry. All complexes were determined for some metabolic enzyme activities. Results indicated that all the synthetic complexes exhibited powerful inhibitory actions against all aims as compared to the control molecules. K_i values of new morpholine-liganded complexes bearing 4-hydroxyphenylethyl group **1a-e** for hCA I, hCA II, AChE, BChE, and α-glycosidase enzymes were obtained in the ranges 0.93–2.14, 1.01–2.03, 4.58–10.27, 7.02–13.75, and 73.86–102.65 µM, respectively. Designing of reported complexes is impacted by molecular docking study, and interaction with the current enzymes also proclaimed that compounds **1e** (−12.25 kcal/mol for AChE and −11.63 kcal/mol for BChE), **1c** (−10.77 kcal/mol and −9.26 kcal/mol for α-Gly and hCA II, respectively), and **1a** (−8.31 kcal/mol for hCA I) are showing binding affinity and interaction from the synthesized five novel complexes.

KEYWORDS
enzyme inhibition, molecular docking, XRD, morpholine, *N*-heterocyclic carbene, palladium, phenol

1 | INTRODUCTION

N-heterocyclic carbenes (NHCs) have attracted the attention of chemists as unique ligands in the field of organic and organometallic chemistry for a long time.[1] Diverse applications of these ligands come to light day by day. Many research groups have made NHC indispensable in various research areas such as organocatalysis,[2,3] homogeneous catalysis,[4,5] materials science,[6,7] and even medicinal chemistry.[8,9] Electronically and sterically adjustability of NHC ligands and their stable complexation with transition metals are among the most important properties of these ligands.[10,11] Transition metal complexes of NHC ligands (M-NHC), which originally emerged as active catalysts, have been the topic of numerous studies in this field. M-NHC complexes comprising Pt,[12] Ru,[13] Ag,[14] Au,[15] Cu,[16] and Pd[17–20] have been confirmed to be bioactive over the last two decades. Recently, new studies on the medicinal

 © 2023 Wiley Periodicals LLC.

applications of M-NHC complexes containing benzimidazole ligand have been published.[21,22] It is clear why organic and organometallic chemists are interested in these complexes from the successful outcomes of the numerous applications (mentioned above) of these compounds.

Phenolic compounds are in the class of bioactive compounds. Polyphenols are considered natural antioxidants and also exhibit diverse biological activities when it comes to human health,[23] such as antimicrobial, antidiabetic, antioxidants, and anti-inflammatory.[24,25] Morpholine, another class of compounds, is a heterocyclic compound often used in medicinal chemistry due to its advantageous physicochemical, and biological properties as well as its mostly easy synthetic pathways. Nitrogen-containing heterocycles such as morpholine derivatives have been extensively researched by organic chemists for their close relationship with diverse biological activities and clinical applications in the treatment of some diseases.[26] It has long been known that suitably substituted morpholine has a wide range of biological effects, such as antioxidant, antimicrobial, antiobesity, analgesic, anti-inflammatory, antihyperlipidemic, antineurodegenerative, and anticancer activities.[27–29] After 1955, important work was carried out to discover the large biological activity spectrum of morpholine-containing compounds.[30] The optional arrangement of substituted groups on NHC ligands provides the opportunity to easily modify these ligands. Functional groups substituted on the NHC ligand provide the M-NHC complex with an active site in terms of chemical interaction, while also gaining secondary interaction (such as hydrogen bonding) property. The biological activities of phenolic and morpholine groups in diverse applications are known.[24,25,29] Furthermore, these groups contribute to the increase of the solubility of the compounds in water and many other organic polar solvents by imparting hydrophilic properties to the compounds with which they are substituted.

Carbonic anhydrase (CA) is a zinc-containing enzyme that is present in all living things. An essential biological process, the reversible hydration of CO_2 to a bicarbonate ion and a proton, is catalyzed by this enzyme family. In addition to homeostasis, CA is very important for lipogenesis, gluconeogenesis, maintenance of normal physiological pH balance, and ureogenesis.[31] Indeed, in vertebrates, including human cells, α-CAs have a variety of isoforms, and 16 various isoforms of CA have been recorded in humans. Overexpression of certain CA isozymes is responsible for different ailments and some diseases such as glaucoma, cancer, osteoporosis, obesity, and epilepsy. CA inhibitors are first-line treatments for osteoporosis, glaucoma, cancer, neurological disturbances, and obesity, as well as duodenal and gastric ulcers; these can also act as antiepileptics. CA inhibitors have the power to open up capillaries in the retina and prevent obstruction.[32]

Alzheimer's disease (AD) is a neurological condition that affects senior populations and is characterized by dementia, memory loss, and cognitive impairment. The neurotransmitter acetylcholine (ACh) is hydrolyzed at cholinergic synapses in both the peripheral and central nervous systems by the acetylcholinesterase enzyme (AChE). The progression of AD has been observed to be complex and associated with multiple cues such as destruction of cholinergic nerves in the brain, decreased ACh levels, dyshomeostasis of metal ions, oxidative stress, accumulation of amyloid-β plaques, mitochondrial malfunction, and others.[33]

The α-glycosidase enzyme is a significant metabolic enzyme located on the brush surface of the small intestine. Diabetes treatment includes noninsulin and insulin-dependent therapy. Insulin sensitizers (thiazolidinediones and biguanides), α-glycosidase inhibitors (miglitol and acarbose), secretagogues (glinides and sulfonylureas), incretins (DPP-4 inhibitors and GLP-1 receptor agonists), bromocriptine, pramlintide, and sodium-SGLT (co) −2) inhibitors are noninsulin treatments, while insulin treatments include insulin analogs.[34] This work evaluates the α-glycosidase inhibition impacts of new complexes that can lead to the recovery of postprandial hyperglycemia and reconnaissance of new hCA inhibitors to control the impacts of glaucoma, cancer, and neurological disturbances.[35]

The molecular docking technique is useful for atomic-level molecular modeling of the interaction between a tiny complex acting as the ligand and one or more proteins acting as the target(s). As a result, the main metabolic processes and the orientations of small molecules in the binding region of target proteins can be illuminated.[36] There are only two simple steps in the docking process. These include a description of the ligand's conformation and an assessment of the nature of their interaction.[37] The best poses of five newly synthesized compounds (1a-e) and their binding energies against the target enzymes have been used to define the relative two descriptors in the docking approach in the current study. Indeed, AChE, BChE, hCA I and II, and α-glycosidase (α-Gly) are discussed in forthcoming sections of the study.

There have been several studies using palladium-based M-NHC complexes as enzyme inhibitors.[38] Also, our working group has informed studies about the enzyme inhibition activities of the Pd(II) NHC complexes containing diverse functional group-substituted NHC ligands.[39] Recently, our working group researched the enzyme inhibition effects of benzimidazolium-based PEPPSI (Pyridine Enhanced Precatalyst Preparation Stabilization and Initiation)-type Pd(II)NHC complexes bearing cyanobenzyl,[38] phthalimide,[39] and hydroxyethyl[40] functional groups. The PEPPSI-type Pd(II)NHC complexes bearing the cyanobenzyl group exhibited values in the range of 0.325–0.707, 0.238–0.636, and 0.576–1.693 μM against hCA I, hCA II, and XO, respectively.[21] Also, the complexes bearing the phthalimide group inhibited AChE, with Ki values in the range of 0.54 ± 0.10–3.01 ± 0.63 μM, and inhibited BChE, with Ki values in the range of 0.82 ± 0.11–5.03 ± 0.86 μM. For α-Gly, the most effective Ki values of 23.83 ± 5.98.[38] The complexes bearing the hydroxyethyl group exhibited Ki values in the range of 13.77 ± 2.21–30.81 ± 4.87 nM against hCA II, 5.78 ± 0.33–22.51 ± 8.59 nM against hCA I, 3.25 ± 0.34–12.89 ± 4.77 nM against BChE, and 0.44 ± 0.08–1.87 ± 0.11 nM against AChE.[39] The literature on the biological activity of substances containing morpholine and phenolic groups was previously highlighted. The beneficial physical, chemical, biological, and metabolic characteristics of the morpholine ligand, which are often utilized in medicinal chemistry, led us to choose it. In addition, the inhibitory properties of these complexes can be affected by both the

10990461, 0, Downloaded from https://onlinelibrary.wiley.com/doi/10.1002/jbt.23554 by Dokuz Eylul University, Wiley Online Library on [24/10/2023]. See the Terms and Conditions (https://onlinelibrary.wiley.com/terms-and-conditions) on Wiley Online Library for rules of use; OA articles are governed by the applicable Creative Commons License

acidic properties (primary interactions) and the H-bond interaction (secondary interactions) of NHC ligands containing phenol groups. So, here, we report the synthesis of a new series of M-NHC complexes containing both morpholine and phenol-substituted NHC ligand. We characterized all compounds using NMR (^{1}H and ^{13}C), FTIR spectroscopic, and elemental analysis techniques. Furthermore, we have examined the single crystal of **1b** with the X-ray diffraction method. This piece of research portrayed the synthesis, in vitro, and in silico screening of novel complexes for AChE, BChE, carbonic anhydrase I, II, and *α*-glycosidase enzymes.

2 | EXPERIMENTAL

2.1 | General methods

Standard Schlenk methods were used to create all new complexes under inert circumstances. No purification was performed on any of the reagents or solvents before use. These solvents and chemicals were bought from reputable vendors like Abcr, Isolab, and Merck Chemical Company. PEPPSI-type Pd(II)NHC complexes bearing the 4-hydroxyphenylethyl group used as starting materials[40] were synthesized in the organic and organometallic chemistry laboratory of Inonu University, Faculty of Arts and Sciences, Department of Chemistry. Additionally, the Electrothermal-9200 melting point apparatus was used to test the melting points of all complexes in the absence of air using glass capillaries. The 400–4000 cm^{-1} FT-IR spectra experiments were recorded using the Perkin Elmer Spectrum 100 FTIR spectrometer. Carbon (^{13}C) and proton (^{1}H) NMR spectra were saved using a Bruker Avance III 400 MHz NMR spectrometer set to 100 MHz (^{13}C) and 400 MHz (^{1}H) in $CDCl_3$ with tetramethylsilane as an internal reference. Inonu University Scientific and Technology Centre performed the elemental analysis experiment for all complexes.

2.2 | Molecular docking

Docking simulations were implemented based on the biological results of new molecules (Figures 4–8) toward different targets such as AChE, BChE, hCA I, hCA II, and α-Gly. First, the current molecules as ligands were sketched and geometry optimization was done at DFT/B3LYP/SDD level using Gaussian 09 (G09).[41] Density-functional theory (DFT) was employed, which simplifies the computation of physicochemical features of the new molecules at the atomic level, with good correctness and low computational expenditures. The Protein Data Bank (PDB) (www.rcsb.org) was used to obtain the model structures for the four enzymes in question. The model structures were 4EY6 for AChE, 1P0I for BChE, 1AZM for hCA I, and 3HS4 for hCA II. The crystal structure of the isomaltase/-methylglucosidase from *Saccharomyces cerevisiae* (PDB ID: 3AJ7) was used to construct the homology model of the enzyme (EC 3.2.1.20, maltase). Detailed information is also given in Supporting Information.[42–44]

The computational docking program Autodock Vina[45] was utilized to nonbonding interplays between the respective molecules and target proteins. Based on their biological efficiency results, the best modes of only chosen **1a**, **1c**, and **1e** complexes were visualized and assessed with the help of Discovery Studio (DS) 3.5.[46] These data were checked with standard agents TAC for AChE and BChE enzymes, AZA for hCA I and II isoenzymes, and ACR for α-glycosidase. In the meantime, the obtained findings of the other compounds are listed in the Supporting Information.

2.3 | Crystal structure determination

A single-crystal X-ray structure determination of complex **1b** was performed on a Rigaku Oxford Xcalibur diffractometer with an Eos-CCD area detector using MoKα radiation (λ = 0.71073 Å) from an enhanced X-ray source. CrysAlis^{Pro} program[47] was utilized for data collection and data reduction of X-ray diffraction data. We have used the ShelXT[48] structure solution program with Intrinsic Phasing for crystal structure and space group determination. The SHELXL[49] program was employed for crystal structure refinement and the anisotropic refinement of all nonhydrogen atoms. Calculation and analysis of geometrical results were done with the aid of PLATON software.[50] These programs are integrated into the crystallographic software package OLEX2 system.[51] Additionally, to refine some moieties of the molecule, rigid-bond restrains RIGU were imposed. C8–C11 atoms of the morpholine ring, as well as the aromatic ring (C13–C18), were set to be equal to each other by an EADP constraint instruction. Brief contents of the crystal data, experimental particulars, and refinement conclusions for complex **1b** under consideration are listed in Table 1.

2.4 | Synthesis

2.4.1 | Synthesis of the dibromo[1-{(4-hydroxyphenyl)ethyl}-3-methylbenzimidazol-2-ylidene] morpholinepalladium(II), 1a

For the synthesis of complex **1a**; dibromo[1-{(4-hydroxyphenyl)ethyl}-3-methylbenzimidazol-2-ylidene]pyridinepalladium(II) (120 mg, 0.2 mmol) and morpholine (22 mg, 0.25 mmol) in chloroform (4 mL) were stirred for 12 h at room temperature. Then, excess solvents were evaporated under vacuum. Dichloromethane was used to dissolve the remaining solid mixture (15 mL). The obtained solution was passed through a 1 cm thick silica gel filter. Then, under vacuum, dichloromethane in the final filtrate was evaporated. Pentane was used to clean the remaining solid (2 × 10 mL). The solid was dissolved in dichloromethane and crystallized 1/2 with pentane. The final product was obtained as a yellow solid.[52] Yield: 76%; (92 mg); $\nu_{(CN)}$: 1449 cm^{-1}; $\nu_{(NH)}$: 3259 cm^{-1}. % Anal. calc. for $C_{20}H_{24}Br_2N_3O_2Pd$: C: 39.73; H: 4.00; N: 6.95. Found: C: 39.81; H: 4.06; N: 6.90. ^{1}H NMR (400 MHz, $CDCl_3$); δ 2.74 (s, 1H, $HN_{morpholine}$); 2.97 and 3.32 (m, 4H $-NCH_2CH_2O-$); 3.46 (m, 4H $-NCH_2CH_2O-$); 3.80 (m, 2H, $-NCH_2CH_2C_6H_4(OH)$); 4.15 and 4.19 (s, 3H, $-NCH_3$); 4.79 (m, 2H,

10990461, 0, Downloaded from https://onlinelibrary.wiley.com/doi/10.1002/jbt.23554 by Dokuz Eylul University, Wiley Online Library on [24/10/2023]. See the Terms and Conditions (https://onlinelibrary.wiley.com/terms-and-conditions) on Wiley Online Library for rules of use; OA articles are governed by the applicable Creative Commons License

TABLE 1 Crystal data and experimental details for **1b**.

Formula	$C_{27}H_{31}Br_2Cl_2N_3O_2Pd$
Molecular weight	766.67
Temperature (K)	294(2)
Space group	$P2_1/c$
Crystal system	Monoclinic
a; b; c (Å)	16.5896(15); 8.6045(8); 20.712(4)
α; β; γ (°)	90; 91.301(12); 90
Cell volume ($Å^3$)	2955.8(7)
Z	4
ρ_{calc} (g/cm^3)	1.723
F(000)	1520.0
μ (mm^{-1})	3.542
Crystal size (mm^3)	0.28 × 0.19 × 0.06
Radiation/wavelength (Å)	MoK_α/0.71070
Reflections collected	9287
h, *k*, *l*	−20 ≤ h ≤ 20; −6 ≤ k ≤ 10; −25 ≤ l ≤ 19
Data/restraints/ parameters	5408/12/287
Final R indexes [I ≥ 2σ (I)]	R_1 = 0.0767, wR_2 = 0.1871
Final R indexes [all data]	R_1 = 0.2019, wR_2 = 0.2163
GOOF on F^2	0.849
Largest diff. Peak/hole (e $Å^{-3}$)	1.04/−1.32

–NC*H*$_2$CH$_2$C$_6$H$_4$(OH)); 6.67 and 7.10 (d,d, 4H, *J* = 8.3 Hz and *J* = 7.1 Hz, –C$_6$*H*$_4$(OH)); 7.01–7.27 (m, 5H, –C$_6$H$_4$(O*H*) and Ar-*H*). ^{13}C NMR (100 MHz, $CDCl_3$) δ; 34.8 (–NCH$_2$CH$_2$C$_6$H$_4$(OH)); 35.1 (–NCH$_3$); 48.2 (–NCH$_2$CH$_2$O-); 50.4 (–NCH$_2$CH$_2$C$_6$H$_4$(OH)); 68.2 (–NCH$_2$CH$_2$O-); 109.9, 110.2, 115.6, 123.0, 130.1, and 134.9 (–*C*$_6$H$_4$(OH) and Ar-*C*); 154.8 (*C*-OH); 163.8 (Pd-$C_{carbene}$).

2.4.2 | Synthesis of the dibromo[1-benzyl-3-{(4-hydroxyphenyl)ethyl}benzimidazol-2-ylidene] morpholinepalladium(II), 1b

Complex **1b** was synthesized using the same method as complex **1a**. But dibromo[1-benzyl-3-{(4-hydroxyphenyl)ethyl}benzimidazol-2-ylidene]pyridinepalladium(II) (135 mg, 0.2 mmol) was used instead of dibromo[1-{(4-hydroxyphenyl)ethyl}-3-methylbenzimidazol-2-ylidene]pyridinepalladium(II). Yield: 80% (109 mg); $\nu_{(CN)}$: 1413 cm^{-1}; $\nu_{(NH)}$: 3275 cm^{-1}. % Anal. calc. for $C_{26}H_{28}Br_2N_3O_2Pd$: C: 45.87; H: 4.15; N: 6.17. Found: C: 45.91; H: 4.18; N: 6.14. ^{1}H NMR (400 MHz, $CDCl_3$); δ 2.73 (s, 1H, *H*N$_{morpholine}$); 2.95 and 3.64 (m, 4H –NC*H*$_2$CH$_2$O-); 3.42 (m, 4H –NCH$_2$C*H*$_2$O-); 3.79 (m, 2H, –NCH$_2$C*H*$_2$C$_6$H$_4$(OH)); 4.87 (m, 2H, –NC*H*$_2$CH$_2$C$_6$H$_4$(OH)); 5.98 (dd, *J* = 17.0, 3.4 Hz, 2H, –NC*H*$_2$C$_6$H$_5$); 6.67 and 7.05 (m,d, 4H, *J* = 3.4 Hz –C$_6$*H*$_4$(OH)); 6.93–7.45 (m, 10H, –C$_6$H$_4$(O*H*) and Ar-*H*). ^{13}C NMR (100 MHz, $CDCl_3$) δ; 35.0 (–NCH$_2$CH$_2$C$_6$H$_4$(OH)); 48.0 (–NCH$_2$CH$_2$O-); 50.3 (–NCH$_2$CH$_2$C$_6$H$_4$(OH)); 53.3 (–NCH$_2$C$_6$H$_5$); 68.0 (–NCH$_2$CH$_2$O–); 110.2, 111.4, 115.6, 123.0, 123.1, 123.2, 127.9, 128.0, 128.3, 128.9, 129.0, 130.1, 133.4, 134.0, 134.1, 134.8, 134.9, 135.0, and 135.1 (–C$_6$H$_4$(OH) and Ar-*C*); 154.8 (*C*-OH); 165.1 (Pd-$C_{carbene}$).

2.4.3 | Synthesis of the dibromo[1-{(4-hydroxyphenyl)ethyl}-3-(3-methylbenzyl)benzimidazol-2-ylidene]morpholinepalladium(II), 1c

Complex **1c** was synthesized using the same method as complex **1a**. But dibromo[1-{(4-hydroxyphenyl)ethyl}-3-(3-methylbenzyl)benzimidazol-2-ylidene]pyridinepalladium(II) (138 mg, 0.2 mmol) was used instead of dibromo[1-{(4-hydroxyphenyl)ethyl}-3-methylbenzimidazol-2-ylidene] pyridinepalladium(II). Yield: 73% (102 mg); $\nu_{(CN)}$: 1413 cm^{-1}; $\nu_{(NH)}$: 3389 cm^{-1}. % Anal. calc. for $C_{27}H_{30}Br_2N_3O_2Pd$: C: 46.68; H: 4.35; N: 6.05. Found: C: 46.75; H: 4.41; N: 5.98. ^{1}H NMR (400 MHz, $CDCl_3$); δ 2.25 (s, 3H, –NCH$_2$C$_6$H$_4$(C*H*$_3$)); 2.73 (s, 1H, *H*N$_{morpholine}$); 2.94 (m, 2H –NC*H*$_2$CH$_2$O-); 3.45 (m, 6H –NCH$_2$C*H*$_2$O-); 3.79 (s, 2H, –NCH$_2$C*H*$_2$C$_6$H$_4$(OH)); 4.87 (m, 2H, –NC*H*$_2$CH$_2$C$_6$H$_4$(OH)); 5.94 (dd, 2H, *J* = 13.4, 7.6 Hz, –NC*H*$_2$C$_6$H$_4$(CH$_3$)); 6.67 and 6.98 (d,d, 4H, *J* = 6.0 Hz and *J* = 10.8 Hz, –C$_6$*H*$_4$(OH)); 6.96-7.31 (m, 9H, –C$_6$H$_4$(O*H*) and Ar-*H*). ^{13}C NMR (100 MHz, $CDCl_3$) δ; 20.4 (–NCH$_2$C$_6$H$_4$(CH$_3$)); 34.0 (–NCH$_2$CH$_2$C$_6$H$_4$(OH)); 46.9 (–NCH$_2$CH$_2$O-); 49.4 (–NCH$_2$CH$_2$C$_6$H$_4$(OH)); 52.4 (–NCH$_2$C$_6$H$_4$(CH$_3$)); 67.1 (–NCH$_2$CH$_2$O–); 109.2, 110.4, 114.5, 121.9, 122.0, 122.1, 124.0, 127.8, 128.0, 129.1, 129.2, 129.3, 133.0, 133.1, 133.7, 133.8, 133.9, and 137.6 (–C$_6$H$_4$(OH) and Ar-*C*); 153.5 (*C*-OH); 164.0 (Pd-$C_{carbene}$).

2.4.4 | Synthesis of the dibromo[1-{(4-hydroxyphenyl)ethyl}-3-(4-methylbenzyl) benzimidazol-2-ylidene]morpholinepalladium(II), 1d

Complex **1d** was synthesized using the same method as complex **1a**. But dibromo[1-{(4-hydroxyphenyl)ethyl}-3-(4-methylbenzyl)benzimidazol-2-ylidene]pyridinepalladium(II) (138 mg, 0.2 mmol) was used instead of dibromo[1-{(4-hydroxyphenyl)ethyl}-3-methylbenzimidazol-2-ylidene] pyridinepalladium(II). Yield: 78% (108 mg); $\nu_{(CN)}$: 1445 cm^{-1}; $\nu_{(NH)}$: 3181 cm^{-1}. % Anal. calc. for $C_{27}H_{30}Br_2N_3O_2Pd$: C: 46.68; H: 4.35; N: 6.05. Found: C: 46.65; H: 4.32; N: 6.09. ^{1}H NMR (400 MHz, $CDCl_3$); δ 2.26 (s, 3H, –NCH$_2$C$_6$H$_4$(C*H*$_3$)); 2.73 (s, 1H, *H*N$_{morpholine}$); 2.82 and 2.90 (m, 4H –NC*H*$_2$CH$_2$O-); 3.43 (m, 4H –NCH$_2$C*H*$_2$O-); 3.63 (m, 2H, –NCH$_2$C*H*$_2$C$_6$H$_4$(OH)); 3.73 (t, 2H, *J* = 9.4 Hz, –NC*H*$_2$CH$_2$C$_6$H$_4$(OH)); 5.95 (s, 2H, –NC*H*$_2$C$_6$H$_4$(CH$_3$)); 7.10 and 7.36 (d,d, 4H, *J* = 7.9 Hz and *J* = 8.0 Hz, –C$_6$*H*$_4$(OH)); 6.95–7.19 (m, 9H, –C$_6$H$_4$(O*H*) and Ar-*H*). ^{13}C NMR (100 MHz, $CDCl_3$) δ; 21.2 (–NCH$_2$C$_6$H$_4$(CH$_3$)); 48.3 (–NCH$_2$CH$_2$C$_6$H$_4$(OH)); 51.5 (–NCH$_2$CH$_2$O-); 53.4 (–NCH$_2$C$_6$H$_2$(CH$_3$)); 68.1 (–NCH$_2$CH$_2$O-); 111.5, 123.1, 127.9, 129.5, 131.8, 134.7 and 138.0 (–C$_6$H$_4$(OH) and Ar-*C*); -(*C*-OH); 165.5 (Pd-$C_{carbene}$).

10990461, 0, Downloaded from https://onlinelibrary.wiley.com/doi/10.1002/jhc.23554 by Dokuz Eylul University, Wiley Online Library on [24/10/2023]. See the Terms and Conditions (https://onlinelibrary.wiley.com/terms-and-conditions) on Wiley Online Library for rules of use; OA articles are governed by the applicable Creative Commons License

2.4.5 | Synthesis of the dibromo[1-{(4-hydroxyphenyl)ethyl}-3-(2,4,6-trimethylbenzyl) benzimidazol-2-ylidene]morpholinepalladium(II), 1e

Complex **1e** was synthesized using the same method as complex **1a**. But dibromo[1-{(4-hydroxyphenyl)ethyl}-3-(2,4,6-trimethylbenzyl) benzimidazol-2-ylidene]pyridinepalladium(II) (143 mg, 0.2 mmol) was used instead of dibromo[1-{(4-hydroxyphenyl)ethyl}-3-methylbenzimidazol-2-ylidene]pyridinepalladium(II). Yield: 72% (104 mg); $\nu_{(CN)}$: 1398 cm^{-1}; $\nu_{(NH)}$: 3218 cm^{-1}. % Anal. calc. for $C_{29}H_{34}Br_2N_3O_2Pd$: C: 48.19; H: 4.74; N: 5.81. Found: C: 48.15; H: 4.71; N: 5.86. ^1H NMR (400 MHz, $CDCl_3$); δ 2.23 and 2.27 (s, 9H, $-NCH_2C_6H_2(CH_3)_3$); 2.74 (s, 1H, $HN_{morpholine}$); 2.90 and 3.36 (m, 4H $-NCH_2CH_2O-$); 3.47 (m, 4H $-NCH_2CH_2O-$); 3.80 (t, 2H, J = 8.0 Hz, $-NCH_2CH_2C_6H_4(OH)$); 4.85 (t, 2H, J = 8.0 Hz, $-NCH_2CH_2C_6H_4(OH)$); 5.91 (s, 2H, $-NCH_2C_6H_2(CH_3)_3$); 6.24 (d, 2H, J = 8.4 Hz, $-NCH_2C_6H_2(CH_3)_3$); 6.24 and 7.15 (d,d, 4H, J = 8.4 Hz and J = 8.4 Hz, $-C_6H_4(OH)$); 6.79–7.19 (m, 5H, $-C_6H_4(OH)$ and Ar-*H*). ^{13}C NMR (100 MHz, $CDCl_3$) δ; 19.9 and 20.1 ($-NCH_2C_6H_2(CH_3)_3$); 33.7 ($-NCH_2CH_2C_6H_4(OH)$); 47.2 ($-NCH_2CH_2O-$); 49.4 ($-NCH_2CH_2C_6H_4(OH)$); 49.7 ($-NCH_2C_6H_2(CH_3)_3$); 67.2 ($-NCH_2CH_2O-$); 109.0, 110.3, 114.5, 121.6, 121.9, 126.3, 128.6, 129.1, 129.4, 133.5, 133.7, 137.7, and 137.8 ($-C_6H_4(OH)$ and Ar-*C*); 153.5 (*C*-OH); 163.2 (Pd-$C_{carbene}$).

2.5 | Bioactivity studies

2.5.1 | hCA isoenzymes inhibition studies

The hCA I and II isoenzymes were purified using Sepharose-4B-L-Tyrosine-sulfanilamide affinity column chromatography for the hCA inhibition experiment.[32] Verpoorte et al.[53] developed a spectrophotometric approach for determining the inhibitory activities of novel benzimidazolium salts carrying 4-hydroxyphenylethyl group **1a-e**, and this method was based on earlier investigations.[54,55]

2.5.2 | AChE/BChE inhibition studies

The novel benzimidazolium salts carrying 4-hydroxyphenylethyl group **1a-e** were tested for their ability to inhibit AChE and BChE using Ellman's method,[56] which was based on earlier research.[57] At a wavelength of 412 nm, the spectrophotometric evaluation of these enzyme inhibitors was conducted.[57]

2.5.3 | α-glycosidase inhibition studies

The reported procedure by Tao et al.[58] was used to determine the novel benzimidazolium salts containing 4-hydroxyphenylethyl group **1a-e** salts' α-glycosidase inhibitory properties. At 405 nm, the absorbance was determined spectrophotometrically.

2.5.4 | ChEs and α-gly inhibition assay

The assays of the AChE and BChE activities were performed by a modified version of Ellman's method,[56] and the inhibitory effect of novel benzimidazolium salts carrying 4-hydroxyphenylethyl group **1a-e** was examined for the AChE (from electric eel; Sigma C2888, Type V-S) and BChE (from equine serum; Sigma C1057) using acetylthiocholine iodide (ATChI; Sigma 01480), and butrylcholine iodide (BChI; Sigma 20780) as the substrates at pH 8.0 at 37°C. At 412 nm, the activity results were measured spectrophotometrically. As in earlier research, p-nitrophenyl-D-glycopyranoside (pNPG; Sigma N1377) was used

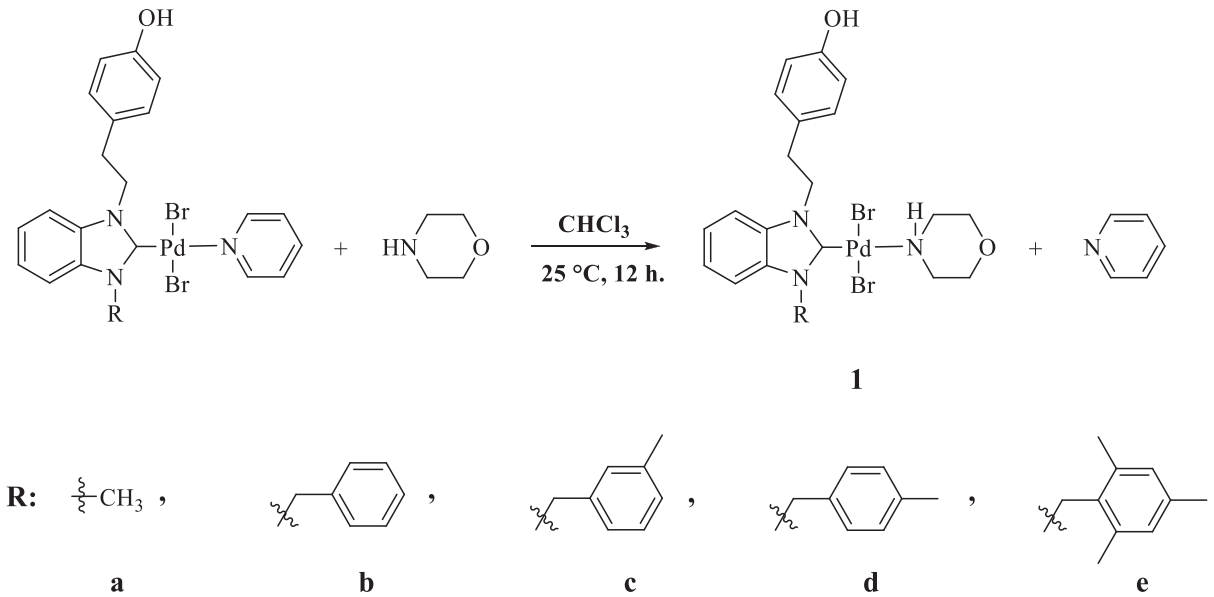

SCHEME 1 Synthesis of the morpholine-liganded Pd(II)NHC complexes (**1a–e**).

10990461, 0, Downloaded from https://onlinelibrary.wiley.com/doi/10.1002/jbt.23554 by Dokuz Eylul University, Wiley Online Library on [24/10/2023]. See the Terms and Conditions (https://onlinelibrary.wiley.com/terms-and-conditions) on Wiley Online Library for rules of use; OA articles are governed by the applicable Creative Commons License

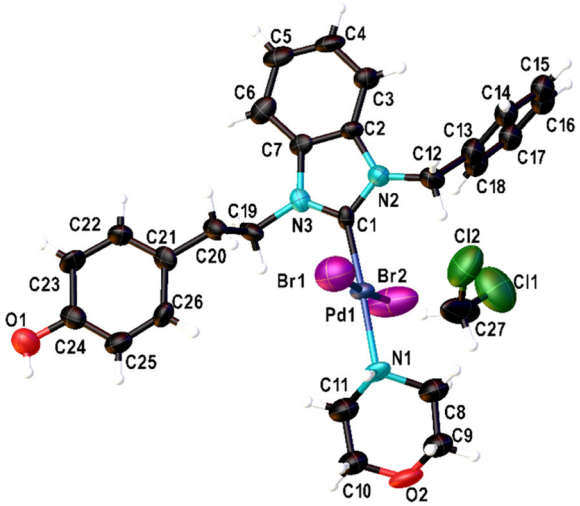

FIGURE 1 The molecular structure of **1b**, showing the atom labeling and the displacement parameters of atoms at the 50% probability level. H atoms are also illustrated as spheres of arbitrary radius. Selected bond parameters (Å,°):O2–C9 1.374(16), O2–C10 1.410(15), N1–C8 1.522(15), N1–C11 1.515(16), N2–C1 1.359(13), N3–C1 1.311(13), Br1–Pd1–Br2 175.87(8), N1–Pd1–Br1 90.3(3), N1–Pd1–Br2 93.1(3), C1–Pd1–Br1 88.6(3), C1–Pd1–Br2 88.1(3), C1–Pd1–N1 177.8(4), N3–C1–N2 107.6(10).

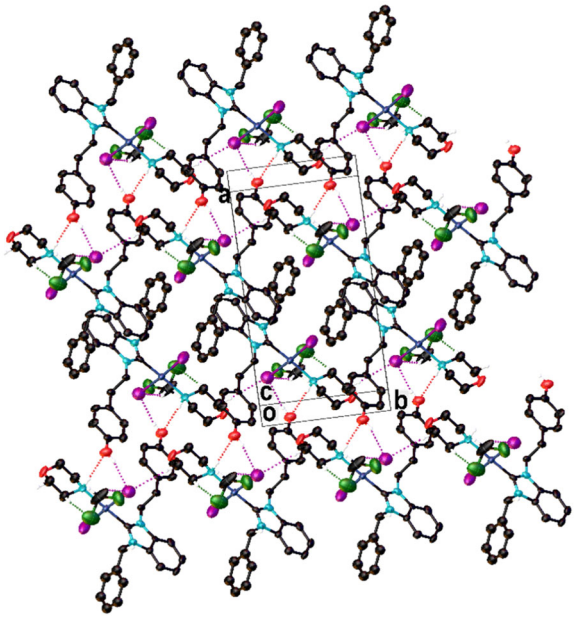

FIGURE 2 A partial view along the *c*-axis of the crystal packing of complex **1b**, showing the intermolecular O–H···Br, N–H···O, and C–H···Br interactions. The intramolecular C–H···Cl and C–H···Br interactions connecting the dichloromethane solvent to the molecule are also shown. H atoms only contributing to interaction have been displayed.

as the substrate at pH 7.4 and 37°C to test the new morpholine-liganded complexes bearing 4-hydroxyphenylethyl group **1a-e**' ability to inhibit α-gly. At 405 nm, the absorbance values were spectrophotometrically determined.[59,60]

2.5.5 | ChEs and α-glu kinetic analysis

At least five distinct inhibitor concentrations were used to investigate the inhibitory effects of new morpholine-liganded complexes bearing 4-hydroxyphenylethyl group **1a-e** on AChE, BChE, and α-gly. According to our prior research, the IC_{50} values of the synthesized compounds were determined from Activity (%)-[Inhibitor] graphs for each derivative. According to earlier investigations, Lineweaver and Burk's curves were used to determine the inhibition types and Ki constants. Results were presented as a mean with a standard error of the mean and 95% confidence intervals. When the $p < 0.05$, differences between data sets were deemed statistically significant.[61,62]

3 | RESULTS AND DISCUSSION

3.1 | Synthesis

This paper describes the synthesis of Pd(II)NHC complexes that incorporate the NHC ligand bearing 4-hydroxyphenylethyl and the morpholine ligand. These new complexes were prepared by mixing 4-hydroxyphenylethyl-substituted PEPPSI-type Pd(II)NHC complexes[40] and morpholine in chloroform (4 mL) at room temperature for 12 h (Scheme 1). Morpholine-ligand Pd(II)NHC complexes were obtained as yellow solids in reasonable yields between 72% and 80%. All complexes are readily soluble in halogenated solvents like dichloromethane and chloroform but less so in polar solvents like water and ethanol. All of the new complexes, however, were insoluble in nonpolar solvents such as toluene and pentane. Spectroscopic methods (^{1}H NMR, ^{13}C NMR, and FTIR) and elemental analysis techniques were used to fully characterize the structures of all complexes. The proposed formula was fully consistent with all spectroscopic data. Proton peaks observed in ^{1}H NMR spectra are stated below. Doublet peaks of the pyridine ligand observed around 9.00 ppm in the starting material 4-hydroxyphenylethyl-

TABLE 2 Hydrogen bonds and other weak interactions for the **1b**.

D – H ··· *A*	*D* – H (Å)	H ··· *A*(Å)	*D* ··· *A*(Å)	*D* – H ··· *A*(°)
C8–H8B···Cl1	0.97	2.79	3.731 (17)	163
C27–H27B···Br1	0.97	2.85	3.71 (2)	150
N1–H1A···Br1	0.98	2.83	3.224 (10)	105
O1–H1···Br1^{i}	0.82	2.39	3.191 (9)	166
C9–H9A···Br1^{ii}	0.97	2.91	3.759 (14)	147
C12–H12B···Cg1^{iii}	0.97	2.92	3.840 (14)	158
C27–H27A···Cg2^{iv}	0.97	2.82	3.68 (2)	148

Note: Symmetry transformations used to generate equivalent atoms: *i*: –x,1–y,1-z; *ii*: x,–1+y,z; *iii*: 1–x,1/2+y,3/2–z; *iv*: x,1/2–y,1/2+z. Cg1 and Cg2 indicate the centroid of (C13–C18) and (C21–C26) rings, respectively.

10990461, 0, Downloaded from https://onlinelibrary.wiley.com/doi/10.1002/jbt.23554 by Dokuz Eylul University, Wiley Online Library on [24/10/2023]. See the Terms and Conditions (https://onlinelibrary.wiley.com/terms-and-conditions) on Wiley Online Library for rules of use; OA articles are governed by the applicable Creative Commons License

substituted PEPPSI-type Pd(II)NHC complexes were not observed in the spectra of these new morpholine-liganded Pd(II)NHC complexes. However, proton peaks of the morpholine ligand (N-*H*) were observed as singlet at 2.73 and 2.74 ppm. Also, proton peaks of the morpholine ligand (–CH_2-) were observed as doublets, triplets, and multiples between 2.90 and 3.80 ppm. Aromatic proton peaks, including the OH proton peaks in the 4-hydroxyphenyl ethyl group, were observed between 6.70 and 7.35 ppm for all complexes. Benzylic CH_2 proton peaks were observed around 5.95 ppm as singlets and double doublets. The peaks of ethyl (CH_2) protons in the 4-hydroxyphenylethyl group were observed as singlet, triplet, and multiplets around 3.80 and 4.80 ppm. While methyl proton peak on nitrogen atom was observed as singlet at 4.19 ppm, methyl proton peaks on the benzene ring were observed as singlet at around 2.25 ppm. The following data were observed for the ^{13}C NMR spectra. In all new complexes **1a-e**, the characteristic carbene peaks (2-$C_{carbene}$) were observed at 163.8, 165.1, 164.0, 165.5, and 163.2 ppm, respectively. Aromatic carbon peaks to which the OH group is attached were observed at around 155 ppm. Also, the characteristic morpholine carbon peaks (*C*-N and *C*-O) in these complexes were observed between 47 and 68 ppm. Other aromatic carbon peaks were observed in the range of 109–138 ppm. The carbon peaks for ethyl CH_2 were observed between 35 and 50 ppm, while the carbon peaks for benzylic CH_2 were

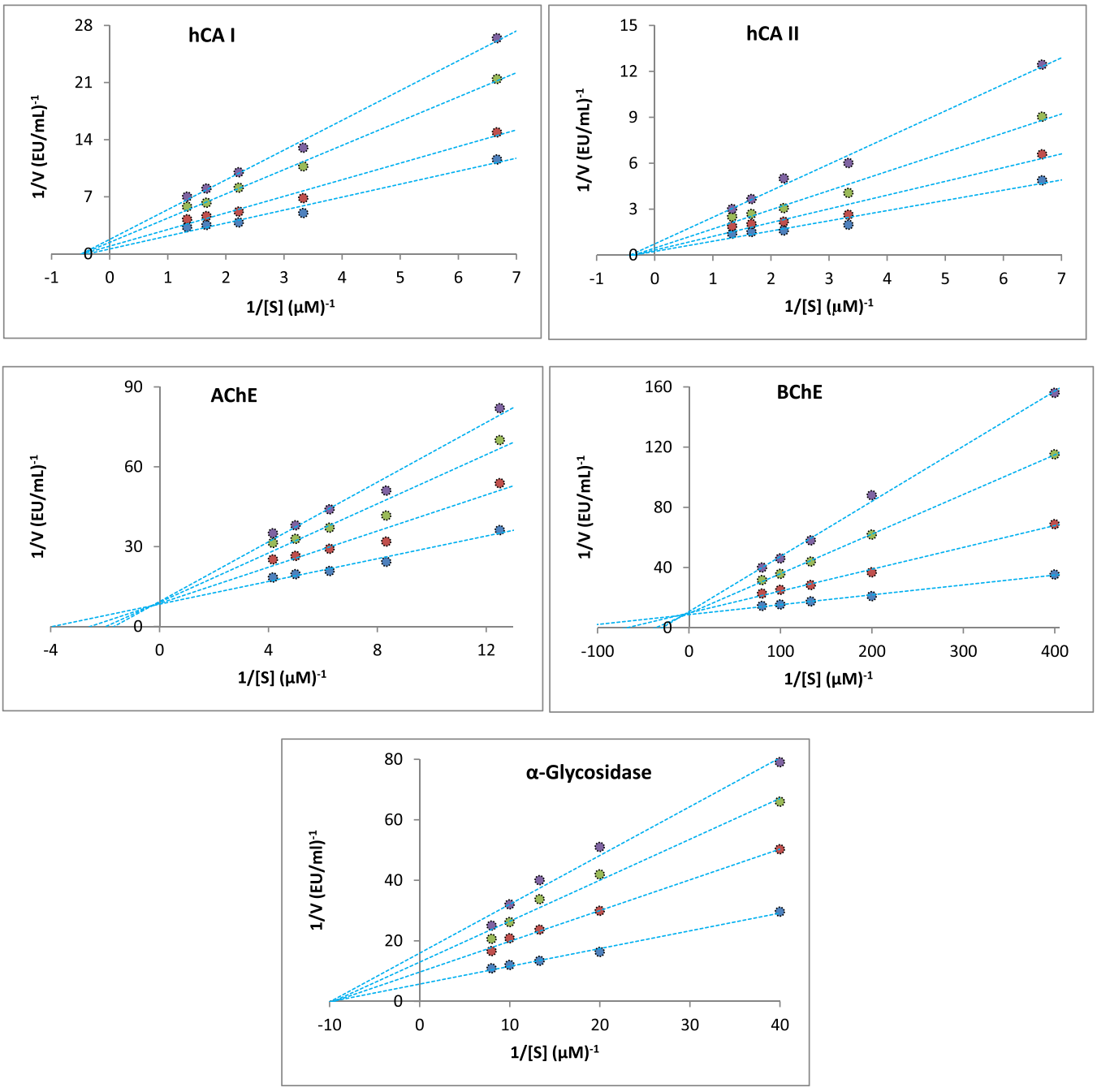

FIGURE 3 Lineweaver–Burk graphs of best inhibitors.

10990461, 0, Downloaded from https://onlinelibrary.wiley.com/doi/10.1002/jbt.23554 by Dokuz Eylul University, Wiley Online Library on [24/10/2023]. See the Terms and Conditions (https://onlinelibrary.wiley.com/terms-and-conditions) on Wiley Online Library for rules of use; OA articles are governed by the applicable Creative Commons License

TABLE 3 In vitro some metabolic enzymes inhibitory activities of novel complexes **1a-e**.

Compounds	IC_{50} (μM)									K_I (μM)				
	hCA I	r^2	hCA II	r^2	AChE	r^2	BChE	r^2	α-Gly	r^2	hCA I	hCA II	AChE	BChE	α-Gly
1a	1.04	0.9672	0.98	0.9516	9.26	0.9672	12.46	0.9561	85.47	0.9812	0.93 ± 0.14	1.04 ± 0.35	8.63 ± 1.02	10.25 ± 2.43	94.37 ± 13.73
1b	1.56	0.9715	1.45	0.9904	15.27	0.9367	16.86	0.9703	100.15	0.9951	1.45 ± 0.20	1.34 ± 0.12	14.27 ± 1.98	13.75 ± 1.87	91.04 ± 12.93
1c	1.27	0.9828	1.20	0.9625	17.33	0.9911	15.98	0.9027	67.47	0.9590	1.16 ± 0.08	1.01 ± 0.10	16.31 ± 2.05	12.55 ± 1.25	73.86 ± 9.51
1d	1.12	0.9615	1.02	0.9691	10.28	0.9889	13.62	0.9625	92.38	0.9162	1.26 ± 0.25	1.18 ± 0.06	9.56 ± 1.11	10.28 ± 1.08	99.10 ± 18.70
1e	1.97	0.9956	1.84	0.9624	5.23	0.9517	7.92	0.9862	98.56	0.9655	2.14 ± 0.15	2.03 ± 0.54	4.58 ± 0.95	7.02 ± 0.94	102.65 ± 14.89
AZA[a]	2.21	0.9901	2.01	0.9819	-	-	-	-	-	-	2.54 ± 0.61	2.18 ± 0.41	-	-	-
TAC[b]	-	-	-	-	18.21	0.9760	23.38	0.9140	-	-	-	-	13.32 ± 2.38	20.12 ± 3.27	-
ACR[c]	-	-	-	-	-	-	-	-	375.38	-	-	-	-	-	436.41

[a]It is a standard compound for hCA I and II.
[b]It is a standard compound for AChE and BChE.
[c]It is standard for α-glycosidase.

TABLE 4 The binding energy of complex **1a-e**, TAC (as the control for AChE and BChE), AZA (as the control for hCA I and hCA II), ACR (as the control for α-Gly), and with the five target enzymes, respectively.

AChE	Free energy of binding (kcal/mol)
1a	−10.04
1b	−11.3
1c	−11.8
1d	−10.56
1e	−12.25
TAC	−7.37
BChE	**Free energy of binding (kcal/mol)**
1a	−9.05
1b	−11.33
1c	−11.35
1d	−11.05
1e	−11.63
TAC	−6.81
hCA I	**Free energy of binding (kcal/mol)**
1a	−8.31
1b	−7.86
1c	−7.89
1d	−7.83
1e	−7.39
AZA	−6.14
hCA II	**Free energy of binding (kcal/mol)**
1a	−8.37
1b	−9.13
1c	−9.26
1d	−9.23
1e	−8.37
AZA	−6.56
α-Gly	**Free energy of binding (kcal/mol)**
1a	−8.71
1b	−9.98
1c	−10.77
1d	−10.46
1e	−10.61
ACR	−7.53

observed around 52 ppm. The methyl carbon peak on the nitrogen atom was 35.2 ppm, while the methyl carbon peaks on the aromatic benzene rings were around 20 ppm. C-N stretching was observed in the FTIR spectra at 1449, 1413, 1413, 1445, and 1398 cm^{-1} for the new

10990461, 0, Downloaded from https://onlinelibrary.wiley.com/doi/10.1002/jbt.23554 by Dokuz Eylul University, Wiley Online Library on [24/10/2023]. See the Terms and Conditions (https://onlinelibrary.wiley.com/terms-and-conditions) on Wiley Online Library for rules of use; OA articles are governed by the applicable Creative Commons License

complexes **1a-e**, respectively. Furthermore, for the new complexes 1a-e, O-H stretching from the phenolic OH group was observed at 3259, 3275, 3389, 3181, and 3218 cm^{-1}, respectively. When the elemental analyzed data were reviewed, it was shown that the calculated values were very close to the found values. All spectral data are compatible with the literature.[40,52,63,64]

3.2 | Structural studies

Figure 1 shows the molecular structure of complex **1b** along with the atom labels. The N atom from the morpholine ring and the C atom from NHC, both of which are in trans position, each occupy two sites in the four-coordinate coordination geometry around the palladium atom, while the two Br atoms occupy the other two sites. The metal coordination environments of complex **1b** adopt a slightly distorted square–planar environment due to the fact that the bond angles around the metal atom which are expected to be 180˚ for idealized square-planar coordination geometry differ only a bit from the ideal case. The Pd atom lies −0.008 Å out of the coordination plane defined by the atoms N1, C1, Br1, and Br2. The benzimidazole and the morpholine rings are nearly perpendicular to the coordination plane $PdBr_2CN$, with a dihedral angle of 88.61 (12)˚ and 88.46 (11)˚, respectively. The two Pd–Br bond distances are a bit different from each other [2.378(2) and 2.397(2) Å] which are slightly smaller than that compared to four–coordinate square–planar palladium(II) complexes.[52,63–71] The bond angles and distances of the morpholine ring are comparable to those reported in the literature.[52,68,69] The morpholine ring exhibits a chair conformation with puckering parameters Q = 0.507(14) Å, θ = 2.0(15)°, and φ = 185(37)°.[70] The $Pd–N_{morpholine}$ and $Pd–C_{carbene}$ bond lengths are 2.144(9) and 1.952(12) Å, and close to the corresponding value reported in the literature.[52]

In the crystal structure of the complex **1b**, the neighboring molecules are connected to one another by a pair of O1–H1···Br1^{i} and N1–H1A···O1^{i} (symmetry code: (*i*) –x,1–y,1–z) hydrogen bond which gives rise to inversion dimers with an $R_2^2(24)$ graph-set motif. These dimer linkages are bonded by intermolecular C9–H9A···Br1^{ii} (symmetry code: (*ii*) x,–1+y,z) hydrogen bonds to create a chain arrangement extending along the *b*-axis of the unit cell. In addition to these hydrogen bonds, links between dimers are aided by C12–H12B···Cg1^{iii} (symmetry code: (*iii*) 1–x,1/2+y,3/2–z)

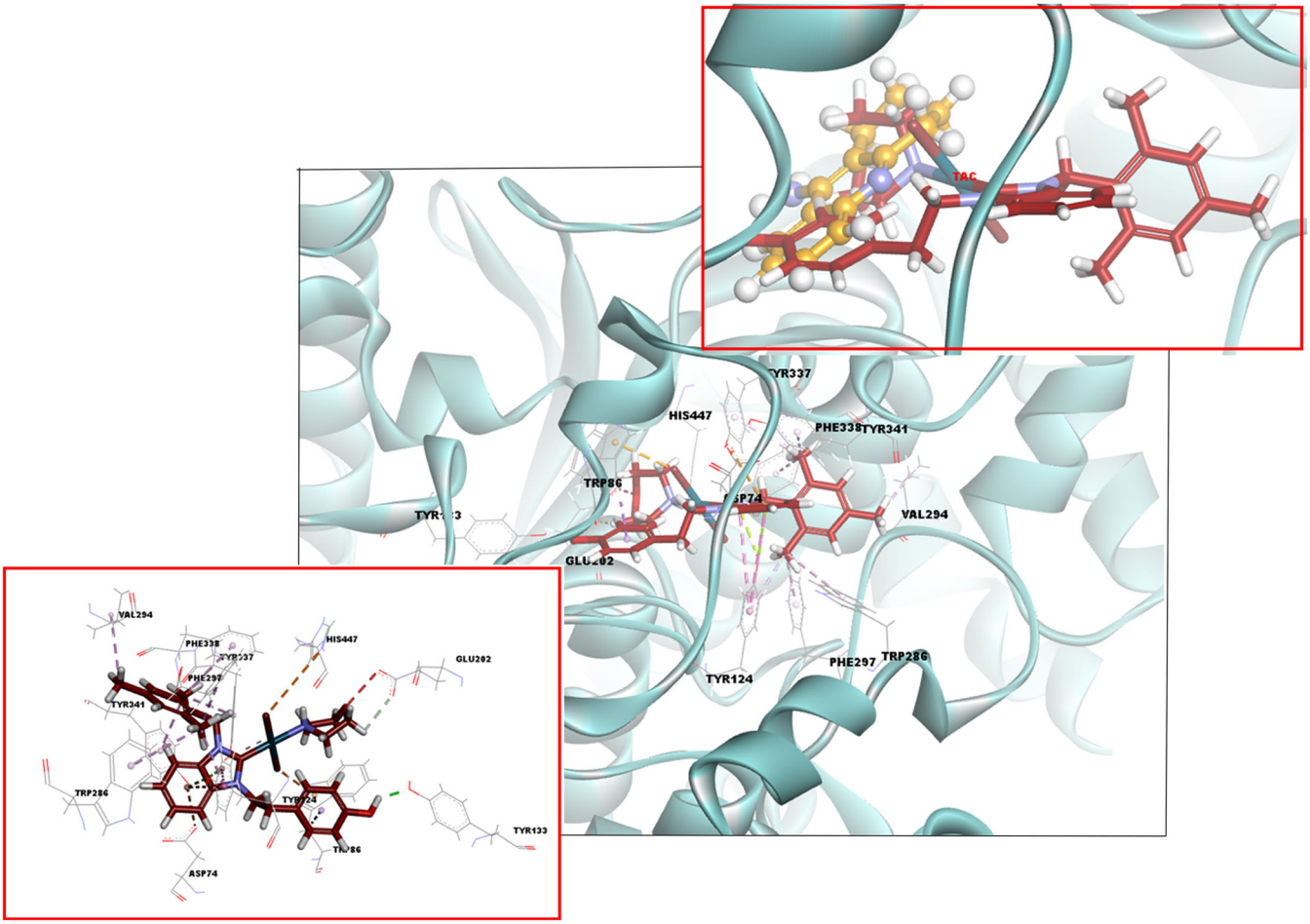

FIGURE 4 3D view of docking interactions of complex **1e** (brown color, stick form) and TAC (orange, ball and stick form) as positive compound with AChE. TAC, tacrine.

10990461, 0, Downloaded from https://onlinelibrary.wiley.com/doi/10.1002/jbt.23554 by Dokuz Eylul University, Wiley Online Library on [24/10/2023]. See the Terms and Conditions (https://onlinelibrary.wiley.com/terms-and-conditions) on Wiley Online Library for rules of use; OA articles are governed by the applicable Creative Commons License

interactions involving the aromatic rings (C13–C18) as acceptor and H atoms of the methylene group as the donor. As seen in Figure 2, the dichloromethane solvent is linked to molecule through the intramolecular C8–H8B···Cl1 and C27–H27B···Br1 interactions constitute a cyclic dimer with an $R_2^2(8)$ loop. Besides, intermolecular C27–H27A··· $Cg2^{iv}$ interactions (symmetry code: (*iv*) x,1/2−y,1/2+z) are present between hydrogen atom of dichloromethane and aromatic ring (C21–C26), stacking molecules along the *c*-axis. The intramolecular N1–H1A···Br1 interactions are also found between the H atoms upon $N_{morpholine}$ atoms and Br atoms. Finally, the supramolecular cluster is constructed by π–π stacking interactions [$Cg3\cdots Cg3^{v}$ = 3.754 (7) Å, inter-planar distance = −3.468(5) Å, slippage = 1.437 Å, α = 0.0(6)°, symmetry code: (*v*) 1−x,1−y,1−z] between two aromatic (C2–C7) rings. Since the obtained value for the distance between the centroids of these overlapping rings is smaller than the maximum separation for π–π interactions of 3.8 Å, then this result can be regarded a plausible evidence for the presence of π–π interactions in the crystal structure.[71] Table 2 provides complete details of the intra- and intermolecular interactions using symmetry codes.

3.3 | Biochemistry results

In the previous study, the inhibitory actions of hCA I, hCA II, AChE, BChE, and α-Gly were all examined in all complexes.[40] The Tao and Ellman techniques were used to assess the ChE inhibitory activity of the novel PEPPSI-Pd-NHC complexes containing the 4-hydroxyphenylethyl group against α-Gly, AChE, and BChE. The results showed that, when compared to the common inhibitors, all the synthesized complexes demonstrated potent inhibitory actions against all targets, as shown by IC_{50} values. The *Ki* values of the novel PEPPSI-Pd-NHC complexes were determined to be in the ranges of 18.98–32.65, 22.95–38.13, 3.67–11.65, 4.09–9.36, and 186.92–287.45 μM for hCA I, hCA II, AChE, BChE, and α-Gly, respectively.[40] However, our study's findings showed that, as compared to the control molecules, every synthesized complex demonstrated strong inhibitory effects against every objective. For hCA I, hCA II, AChE, BChE, and α-glycosidase enzymes, the *Ki* values of new morpholine-liganded complexes bearing 4-hydroxyphenylethyl group **1a-e** were obtained in the ranges of 0.93–2.14, 1.01–2.03, 4.58–10.27, 7.02–13.75, and 73.86–102.65 μM, respectively.

Herein, complex 1a (hCA I, Ki = 0.93 0.14 μM; IC_{50} = 1.04 μM with r^2: 0.9672) having methyl group was recognized as the most powerful inhibitor of hCA I isoform when compared to the standard acetazolamide (Ki = 2.54 0.61 μM) among all synthetic new morpholine-liganded complexes bearing 4-hydroxyphenylethyl group 1a-e. However, compared to other complexes, analog **1e**, which contains a 2,4,6-trimethylbenzyl group (hCA I, Ki = 2.14 0.15 μM; IC_{50} = 2.21 μM with r^2: 0.9901), shows less inhibitory potential against the target. Comparing the activity of complexes **1c** and **1d** (hCA I, K_i = 1.16 ± 0.08 μM; K_i = 1.26 ± 0.25 μM) reveals that

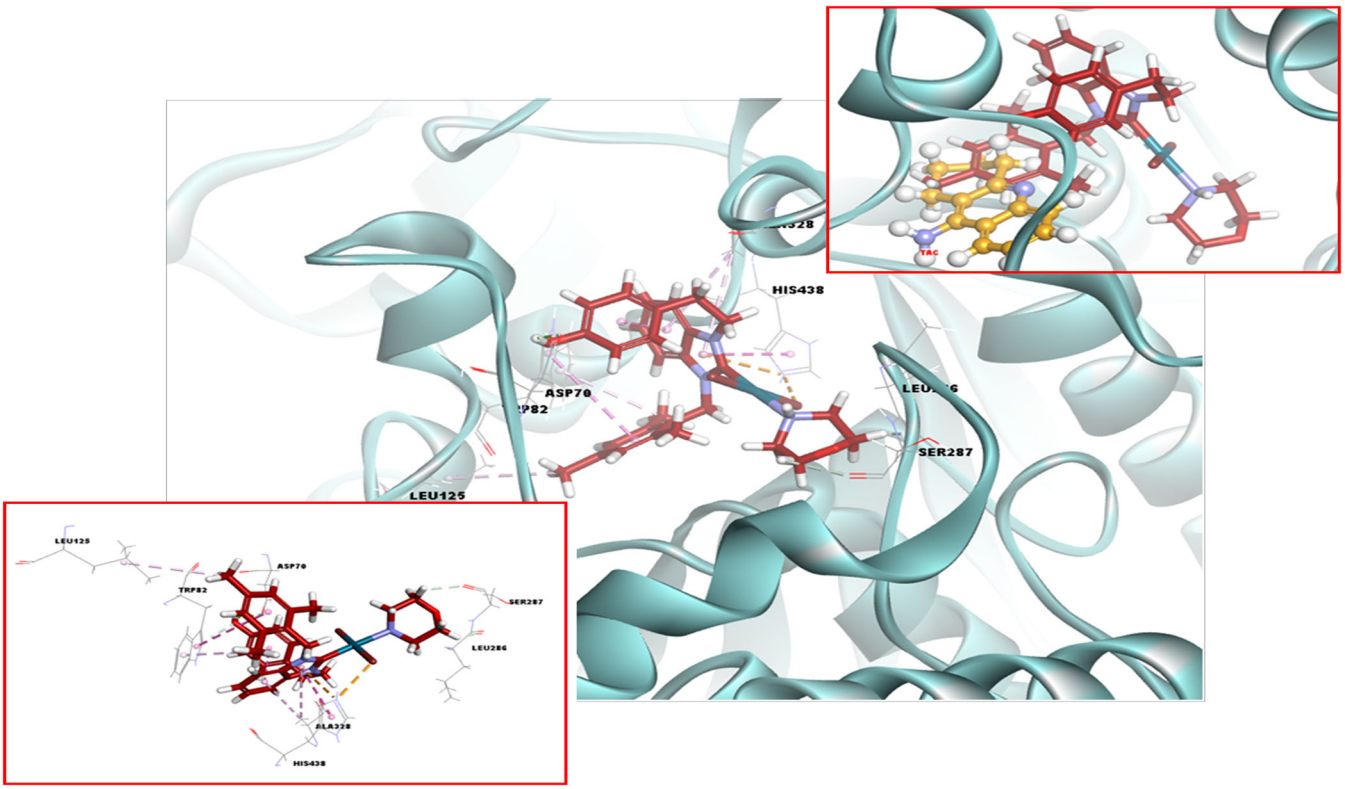

FIGURE 5 3D view of docking interactions of complex **1e** (red color, stick form) and TAC (orange, ball and stick form) as positive compound with BChE.

10990461, 0, Downloaded from https://onlinelibrary.wiley.com/doi/10.1002/jbt.23554 by Dokuz Eylul University, Wiley Online Library on [24/10/2023]. See the Terms and Conditions (https://onlinelibrary.wiley.com/terms-and-conditions) on Wiley Online Library for rules of use; OA articles are governed by the applicable Creative Commons License

switching the position from para- to meta- increases the inhibitory potential against the hCA I isoform. Another complex **1b** (hCA I, K_i = 1.45 ± 0.20 μM; IC_{50} = 1.56 μM with r^2: 0.9715) having benzyl group was the second less potent analog of the series. Nonetheless, the absence of the 3-methylbenzyl group in analog **1c** (hCA II, K_i = 1.01 ± 0.10 μM; IC_{50} = 1.27 μM with r^2: 0.9828) presented the best decrease in hCA II inhibitory potential (Figure 3). Furthermore, all morpholine-liganded complexes bearing 4-hydroxyphenylethyl group **1a**, **1b**, **1d**, and **1e** complexes showed good inhibitory potential against hCA II isoform. Inhibitors of these enzymes are used in the clinical therapy of diverse diseases like acid–base imbalances, different neurological disorders, and glaucoma. The synthesis, characterization, and analysis of CA inhibitors from diverse groups of complexes are very remarkable because of their specificity toward isoenzymes.[72,73] Recently, sulfonamide-based Schiff bases and their metal complexes have been used because of their inhibitory properties against CA I and II isoenzymes. Tacrine served as the positive control, and the anti-cholinesterase effects of new morpholine-liganded complexes bearing 4-hydroxyphenylethyl group **1a-e** were assessed using Ellman's technique. Table 3 lists the IC_{50} and Ki values for the newly synthesized complexes' inhibitory effects against AChE and BChE. As shown in Table 3, the three newly synthesized **1a**, **1d**, and **1e** complexes were more effective than tacrine against AChE, while all of the newly synthesized complexes were more effective than the latter medication against BChE.

The test complexes' K*i* values showed that complex **1e** was the most effective substance against AChE and BChE (AChE, Ki = 4.58 0.95 μM; BChE, K*i* = 7.02 0.94 μM). The inhibitory potential effect was dramatically reduced when the methyl group was replaced with the 2,4,6-trimethylbenzyl group, as in complexes **1a** and **1e**, and when the meta position was changed to the para position, as in complexes **1c** and **1d**, respectively. However, in complexes 1c and 1b, respectively, moving from the 3-methylbenzyl group to the benzyl group resulted in a considerable increase in anti-BChE activity. Complex **1d**, with a K_i of 10.28 M, was the third most effective molecule against AChE among the synthetic derivatives.

In terms of anti-BChE inhibitory potential effect, all complexes bearing 4-hydroxyphenylethyl group **1a-e**, those containing methyl, benzyl, 3-methylbenzyl, 4-methylbenzyl, and 2,4,6-trimethylbenzyl groups, outperformed tacrine. Additionally, cholinesterase inhibitor complexes are very interesting candidate molecules for the extension of drugs for the therapy of some neurological diseases associated

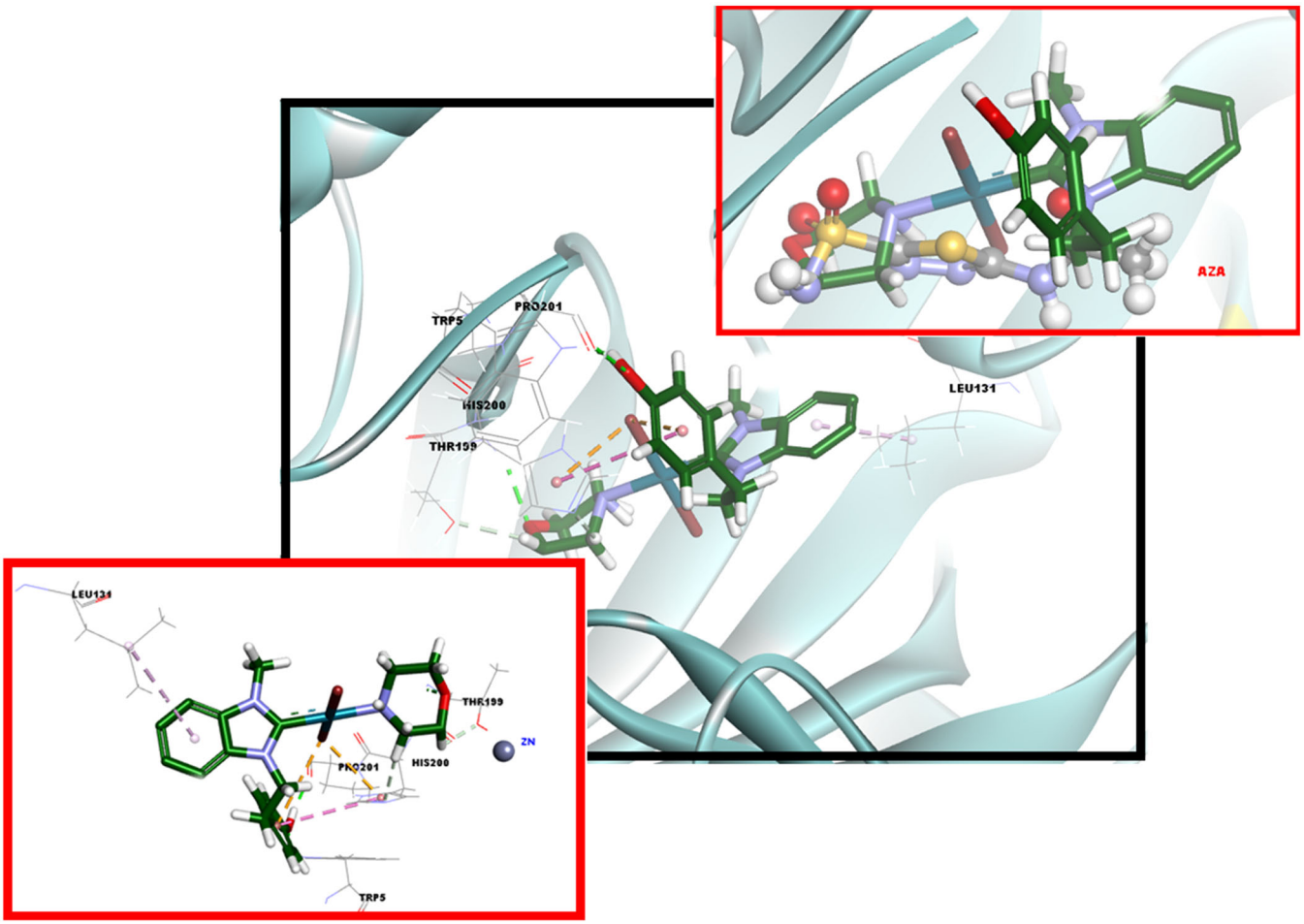

FIGURE 6 3D view of docking interactions of complex **1a** (green, stick form) and AZA (default color, ball and stick form) as positive compound with hCA I.

10990461, 0, Downloaded from https://onlinelibrary.wiley.com/doi/10.1002/jbt.23554 by Dokuz Eylul University, Wiley Online Library on [24/10/2023]. See the Terms and Conditions (https://onlinelibrary.wiley.com/terms-and-conditions) on Wiley Online Library for rules of use; OA articles are governed by the applicable Creative Commons License

with cholinergic transmissions like AD, ataxia, myasthenia gravis, and dementia. Some of these inhibitors, such as tacrine, galantamine, donepezil, and rivastigmine, have recently been used to treat memory loss and cognitive impairment and in individuals with mild to severe AD who have elevated ACh levels in the brain.[74,75]

Complexes that had just been created were also tested against -glucosidase (Table 3). The results showed that various synthetic complexes with K*i* values ranging from 73.869.51 to 102.6514.89 μM exhibited greater inhibitory potential effect than the positive control compound acarbose, which has a K*i* value of 436.41 μM.[76,77] The strongest molecules among the produced complexes were **1c**, having K*i* values of 73.869.51 μM. These complexes were four times as powerful as the acarbose-based positive control. It works by inhibiting the small intestine brush barrier enzyme α-glucosidase competitively, delaying the breakdown of carbohydrates and the absorption of intestinal glucose. These enzymes must work in order for more complicated carbs to release glucose.[78] They thus reduce post-loading insulin production, especially when compared to sulfonylureas, by suppressing postprandial blood glucose. Dextranase, α-amylase, maltase, glucomylase, and sucrose are all inhibited by this substance.[79] Additionally, α-glycosidase inhibitors are used in the treatment of cancer, hepatitis, and HIV. The **1a** and **1b** complexes also showed good inhibitory potential with K_i values of 94.37 ± 13.73 μM and 91.04 ± 12.93 μM against *α*-glucosidase (Figure 3). The **1a**, **1c**, and **1e** complexes showed promising candidate complexes for drug development with considerable in vitro different enzyme inhibitory activities.

3.4 | Molecular docking results

The optimized five molecules were disclosed to docking to describe the interplay between thiazole compounds and the current enzymes. Especially, the **1a**, **1c**, and **1e** complexes have exhibited better activity properties, according to the results of the in vitro part of this research, so that docking procedures were performed via AutoDock Vina. Docked these complexes and examined docking orientation of

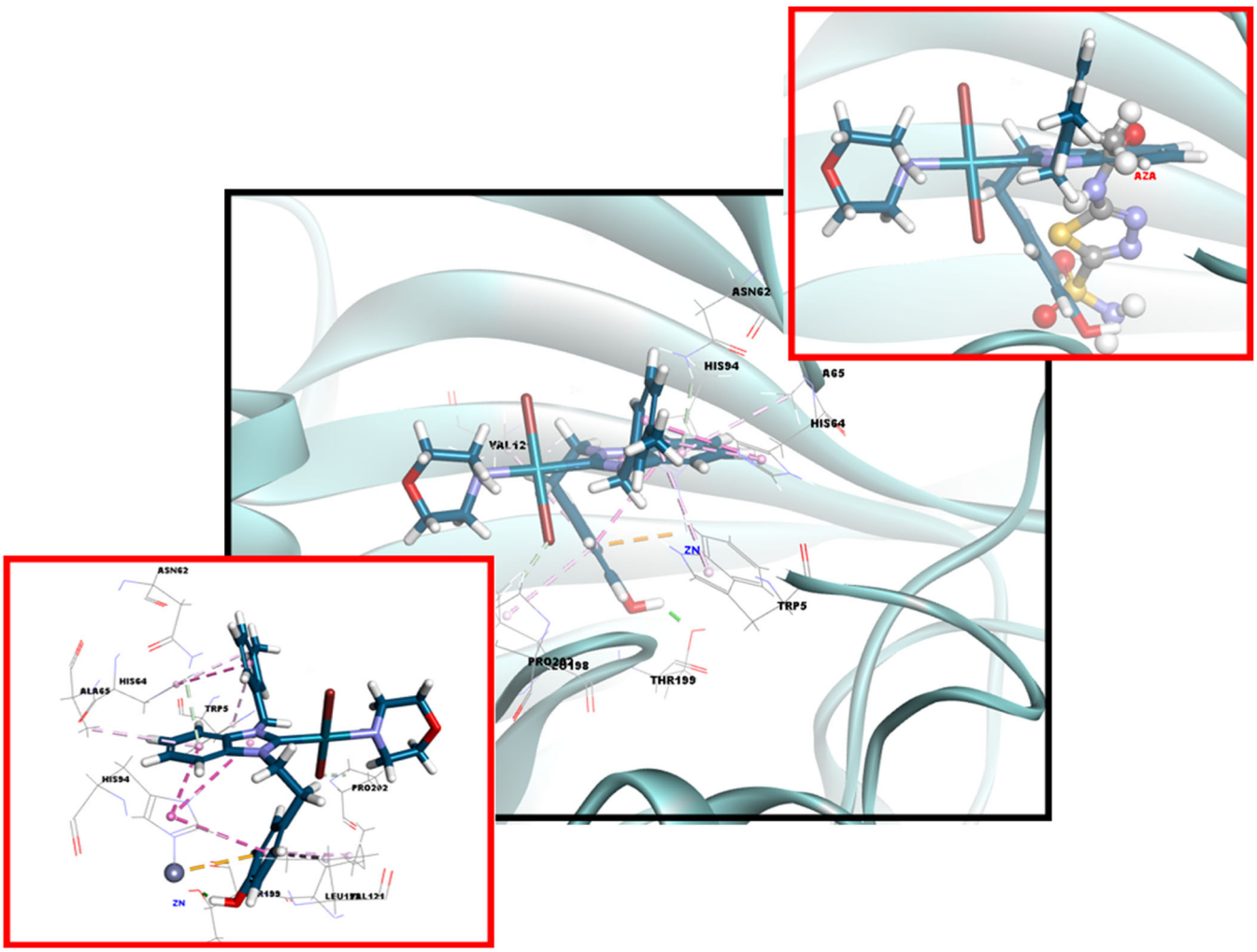

FIGURE 7 3D view of docking interactions of complex **1c** (dark blue, stick form) and AZA (default color, ball, and stick form) as positive compound with hCA II.

10990461, 0, Downloaded from https://onlinelibrary.wiley.com/doi/10.1002/jbt.23554 by Dokuz Eylul University, Wiley Online Library on [24/10/2023]. See the Terms and Conditions (https://onlinelibrary.wiley.com/terms-and-conditions) on Wiley Online Library for rules of use; OA articles are governed by the applicable Creative Commons License

each complex, binding energy and interacting residue of AChE and BChE, hCA I, hCA II, and α-glycosidase are presented in Table 4 and Supporting Information: Table S1. Table 4 presents and evaluates the thermodynamic binding energies of the biological relationships of all synthesized compounds with each target in kcal/mol. In addition, the related compounds are compared with the control compounds (tacrine for AChE and BChE, AZA for hCA I and hCA II, and acarbose for α-glycosidase) of each target, revealing the structure–activity relationship mathematically as well as visual modeling.

As seen in Figure 4, the complex **1e** interaction with Tyr133 (1.958 Å) and Glu202 (2.568 Å) via hydrogen bonding and electrostatic interaction with His447 (5.514 Å) residue and also largely hydrophobic interaction with Asp74 (4.180 Å), Trp86 (3.408, 2.405 Å), Tyr124 (2.899, 2.907, 5.556, 5.439, 4.197 Å), Val294 (4.315 Å), Trp286 (4.873 Å), Phe 297 (3.948 Å), Tyr337 (3.986 Å), Phe338 (4.0142 Å), and Tyr341 (3.690 Å) residues with binding affinity is −12.25 kcal/mol. When the related structure is also compared with tacrine, which is the positive compound of the target enzyme, complex **1e** shows superiority to tacrine (TAC) in terms of both interactions and topological surface width. In this study, the focused region of AChE was included to encompass two distinct binding sites, catalytic action site (CAS) and peripheral anionic site (PAS). The CAS consisted of amino acids Ser203, His447, and Glu334, whereas the PAS consisted of amino acids Tyr72, Asp74, Tyr124, Trp286, and Tyr341. In particular, complex **1e** interacts with the two active sites of the target enzyme, CAS and PAS, thus making it a desirable potential inhibitor candidate Figure (5).

Likewise, it shows the best binding affinity to complex **1e** with the BChE target, and complex **1e** also shows good activity than tacrine with the target. As seen in Table 4 and Figure 4, the binding energy value (−11.63 kcal/mol) of the current compound against BChE is lower than AChE target enzyme. The reason for this is that complex **1e** creates four hydrogen bonds, two electrostatic interactions, and six hydrophobic interactions in the active site of BChE enzyme. In other words, as a result of the close polar–apolar interaction ratio, the efficiency decreased. Similarly, the positive compound, (TAC) interacts less with main residues, with binding affinity value of −6.81 kcal/mol as compared to the complex **1e** structure.

Besides these targets, of the five compounds considered against hCA I and hCA II targets, complex **1a** versus hCA I and complex **1c**

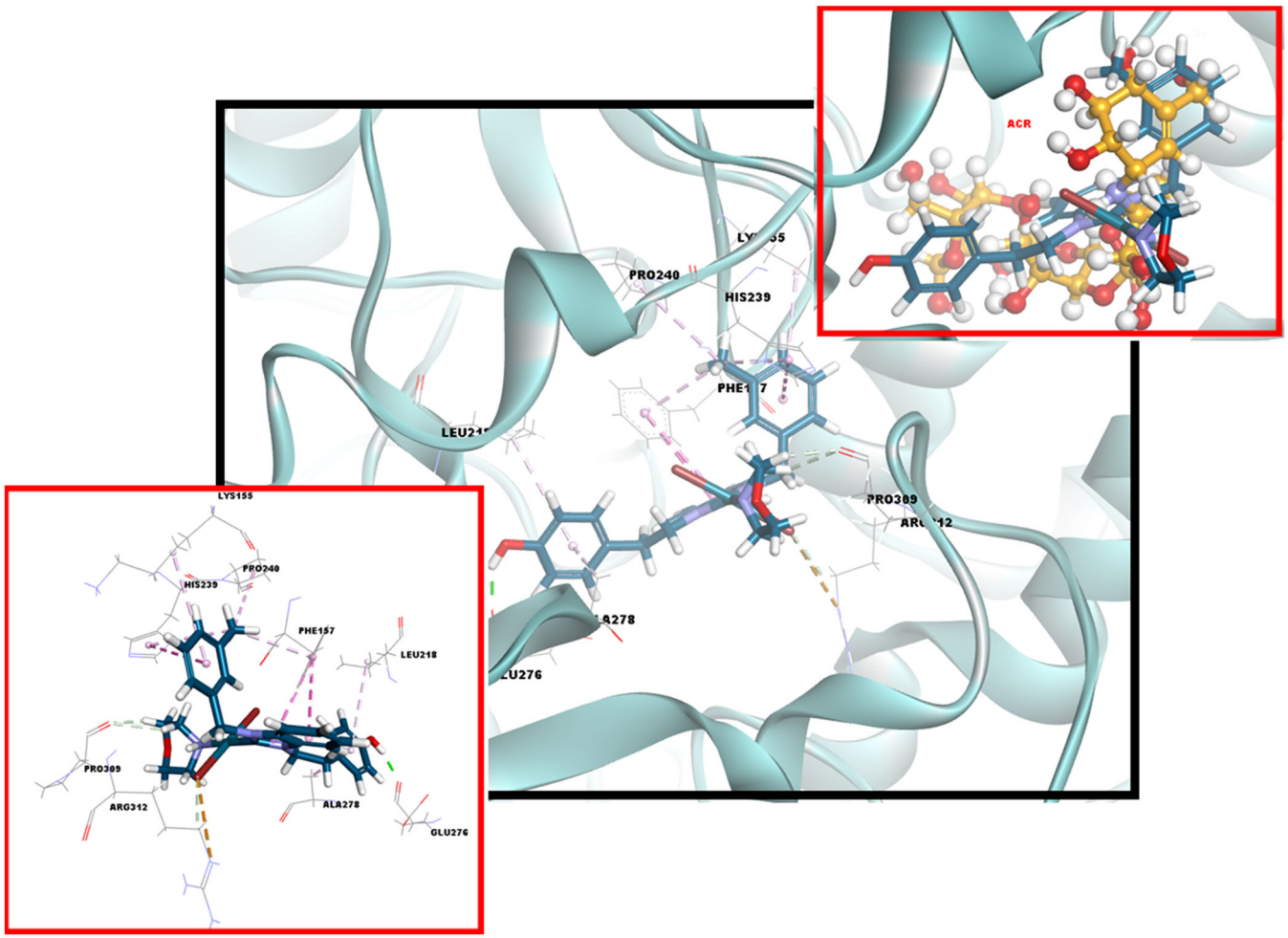

FIGURE 8 3D view of docking interactions of complex **1c** (dark blue stick form) and ACR (orange, ball and stick form) as positive compound with α-Gly.

10990461, 0, Downloaded from https://onlinelibrary.wiley.com/doi/10.1002/jbt.23554 by Dokuz Eylul University, Wiley Online Library on [24/10/2023]. See the Terms and Conditions (https://onlinelibrary.wiley.com/terms-and-conditions) on Wiley Online Library for rules of use; OA articles are governed by the applicable Creative Commons License

against hCA II target have very good binding affinities. When we examine this situation at the atomic level in Figure 6 and Supporting Information: Table S1, complex **1a** has H-bond interaction with residue Trp5 (2.431 Å), Thr199 (2.161 Å), Pro201 (1.848 Å), and His200 (2.567 Å), electrostatic interaction with His200 (3.689 Å), and also hydrophobic interaction with His200 (4.711 Å) and Leu131 (4.592 Å) residues of the hCA I. When we compare it with AZA, the positive compound of the target enzyme, different poses, and interaction differences between complex **1a** and AZA within the same active site, as well as topological surface differences, also differentiate their biological activities against the target (see Supporting Information: Table S1).

Next, complex **1c** exhibits interaction with Thr199 (1.953 Å), Pro202 (2.483 Å), and Asn62 (2.934 Å) via H-bonding and Zn metal (3.840 Å) via electrostatic interaction and also hydrophobic interaction with His64 (4.347 Å), His94 (4.640, 5.569, 4.857 Å), Trp5 (5.0558 Å), Ala65 (4.648 Å), Val121 (5.427 Å), and Leu198 (4.511 Å) residues of hCA II with binding energy value of −9.26 kcal/mol. Whereas, the positive compound, AZA, exhibits dominant way H-bonding with Asn62 (2.300 Å), Thr199 (1.904 Å), His94 (2.774 Å), His96 (2.835 Å), Glu106 (3.0362 Å), Thr200 (2.128 Å), and Leu198 (2.313 Å) and pi-sulfur interaction with His94 (4.838 Å), His96 (5.567 Å), and Trp209 (5.439 Å) residues. This case is shown in Figure 7, and detailed information has been displayed in Supporting Information: Table S1.

Similarly, complex **1c** interacts well with Arg312 (4.825, 2.756 Å), Glu276 (1.980 Å), Pro309 (2.210, 2.854 Å), Phe157 (4.788 Å), His239 (4.918, 4.0391, 4.577 Å), Pro240 (4.907 Å), Leu218 (5.127 Å), Ala278 (2.963 Å), and Lys155 (5.0404 Å), residues of α-Gly, with binding affinity values of −10.77 kcal/mol. On the contrary, acarbose (ACR) as positive compound of the target has H-bonding interaction with Arg212 (2.710, 2.175 Å), Arg241 (2.183, 2.0611, 2.217 Å), Arg439 (1.851, 2.244, 2.333 Å), Ser156 (2.202, 1.901 Å), Glu304 (1.990, 1.777 Å), Glu276 (2.156 Å), Asp68 (2.423, 2.336 Å), His348 (2.319 Å), Asp349 (1.945 Å), and Asp214 (2.0583, 1.848 Å) residues, with binding affinity value of −7.53 kcal/mol. In particular, the common amino acid Glu276, with which the target control compound and complex **1c** interact, exhibits an H-bond interaction with complex **1c** at a distance of 1.980 Å, while the positive compound interacts with the same amino acid at a distance of 2.156 Å. This indicates that the complex **1c** to the target enzyme has a more effective and better interaction than ACR. It is also revealed that hydrophobic interactions appear to predominate over hydrophilic interactions for α-Gly as given in Figure 8.

4 | CONCLUSIONS

As a result, new Pd(II)NHC complexes with morpholine ligands were synthesized in this study. By combining elemental analytical methods with ^{1}H NMR, ^{13}C NMR, and FTIR spectroscopic approaches, the structures of all complexes were thoroughly described. Doublet peaks of the pyridine ligand observed around 9.00 ppm in the starting material PEPPSI-type Pd(II)NHC complexes were not observed in the spectra of the new morpholine-liganded Pd(II)NHC complexes, whereas proton peaks of the morpholine ligand (N-H) were observed as singlet around 2.74 ppm. The characteristic carbene peaks (2-$C_{carbene}$) were observed around 165 ppm for all complexes. In the FTIR spectra, the C-N stretching was observed between 1398 and 1445 cm^{-1} for all complexes. The molecular and crystal structures of 1b have been established through the single-crystal X-ray diffraction method. Structural analysis indicated that palladium atom deviating −0.008 Å from the average Pd–N–C–Br–Br coordination plane adopt a slightly distorted square-planar coordination environment. In the crystal structure, the molecules are connected by intermolecular O–H···Br, N–H···O, and C–H···Br hydrogen bonds. Withal, the crystal packing of **1b** is consolidated via intermolecular C–H···π along with π···π interactions. **1a**, **1c**, and **1e** complexes appear to have the most significant binding affinities and strong contacts with the relevant residues, according to the molecular docking analysis, suggesting that they could be potential inhibitors of the present targets. AChE and BChE, hCA I, hCA II, and α-glycosidase are just a few of the enzymes that certain methyl groups at the fourth and second or third positions on the phenyl part of the main framework will be effective against. This conclusion can be drawn by comparing structure with a biological evaluation of the complexes.

ACKNOWLEDGMENTS

This work is supported by the Scientific Research Projects Commission, Bartin University, Bartin-TURKEY (Project No: 2020-FEN-B-005). The authors thank the Inonu University Faculty of Science Department of Chemistry for the characterization of compounds. The authors thank Esin Akı Yalcin and the research group for technical assistance. The authors thank the Dokuz Eylül University for the use of the Oxford Rigaku Xcalibur Eos Diffractometer (purchased under University Research Grant No: 2010.KB.FEN.13).

CONFLICT OF INTEREST STATEMENT

The authors declare no conflict of interest.

DATA AVAILABILITY STATEMENT

The data that support the findings of this study are available from the corresponding author upon reasonable request. The supplementary crystallographic data for complex **1b** has been deposited to the Cambridge Crystallographic Data Centre (www.ccdc.cam.ac.uk/data_request/cif, e-mail: deposit@ccdc.cam.ac.uk) and is available on request quoting the deposition number CCDC 2089331. Samples of the compounds are available from the authors.

ORCID

Parham Taslimi http://orcid.org/0000-0002-3171-0633
Tuğba Taskın-Tok https://orcid.org/0000-0002-0064-8400
Aydın Aktaş http://orcid.org/0000-0001-8496-6782
Yetkin Gök http://orcid.org/0000-0003-3993-7733
İlhami Gülçin http://orcid.org/0000-0001-5993-1668

10990461, 0, Downloaded from https://onlinelibrary.wiley.com/doi/10.1002/jbt.23554 by Dokuz Eylul University, Wiley Online Library on [24/10/2023]. See the Terms and Conditions (https://onlinelibrary.wiley.com/terms-and-conditions) on Wiley Online Library for rules of use; OA articles are governed by the applicable Creative Commons License

REFERENCES

[1] S. Díez-González, N. Marion, S. P. Nolan, *Chem. Rev.* **2009**, *109*, 3612.
[2] D. Enders, O. Niemeier, A. Henseler, *Chem. Rev.***2007**, *107*, 5606.
[3] N. Marion, S. Díez-González, S. P. Nolan, *Angew. Chem. Int. Ed.* **2007**, *46*, 2988.
[4] A. J. Arduengo, R. L. Harlow, M. Kline, *J. Am. Chem. Soc.* **1991**, *113*, 361.
[5] W. A. Herrmann, C. Köcher, *Angew. Chem., Int. Ed. Engl.* **1997**, *36*, 2162.
[6] L. Mercs, M. Albrecht, *Chem. Soc. Rev.* **2010**, *39*, 1903.
[7] A. J. Boydston, K. A. Williams, C. W. Bielawski, *J. Am. Chem. Soc.* **2005**, *127*, 12496.
[8] W. Liu, R. Gust, *Chem. Soc. Rev.* **2013**, *42*, 755.
[9] M. G. Karaaslan, A. Aktaş, C. Gürses, Y. Gök, B. Ateş, *Bioorg. Chem.* **2020**, *95*, 103552.
[10] P. De Femont, N. Marion, S. P. Nolan, *Coord. Chem. Rev.* **2009**, *253*(7–8), 862.
[11] T. Scattolin, S. P. Nolan, *Trends Chem.* **2020**, *2*(8), 721.
[12] T. Scattolin, G. Valente, L. Luzietti, M. Piva, N. Demitri, I. Lampronti, R. Gambari, F. Visentin, *Appl. Organomet. Chem.* **2021**, *35*(12), e6438.
[13] Y. Sarı, C. Gürses, D. B. Celepci, Ü. Keleştemur, A. Aktaş, Ş. Yüksel, B. Ateş, Y. Gök, *J. Mol. Struct.* **2020**, *1202*, 127355.
[14] A. Behçet, A. Aktaş, Y. Gök, R. Kaya, P. Taslimi, İ. Gülçin, *J. Heterocycl. Chem.* **2021**, *58*(2), 603.
[15] M. Gil-Moles, U. Basu, R. Bessing, H. Hoffmeister, S. Terck, A. Varchmin, I. Ott, *Chem. Eur. J.* **2020**, *26*, 15140.
[16] B. Naderizadeh, M. Bayat, *Mendeleev Commun.* **2021**, *31*, 179.
[17] S. Bal, Ö. Demirci, B. Şen, P. Taslimi, A. Aktaş, Y. Gök, M. Aygün, İ. Gülçin, *Polyhedron* **2021**, *198*, 115060.
[18] T. Scattolin, I. Pessotto, E. Cavarzerani, V. Canzonieri, L. Orian, N. Demitri, C. Schmidt, A. Casini, E. Bortolamiol, F. Visentin, F. Rizzolio, S. P. Nolan, *Eur. J. Inorg. Chem.* **2022**, *2022*(16), e202200103.
[19] T. Scattolin, V. A. Voloshkin, F. Visentin, S. P. Nolan, *Cell Rep. Phys. Sci.* **2021**, *2*(6), 100446.
[20] T. Scattolin, E. Bortolamiol, F. Visentin, S. Palazzolo, I. Caligiuri, T. Perin, V. Canzonieri, N. Demitri, F. Rizzolio, A. Togni, *Chem. Eur. J.* **2020**, *26*(51), 11868.
[21] F. Türker, S. A. A. Noma, A. Aktaş, K. Al-Khafaji, T. Taşkın Tok, B. Ateş, Y. Gök, *Monatsh. Chem.* **2020**, *151*, 1557.
[22] T. Scattolin, A. Piccin, M. Mauceri, F. Rizzolio, N. Demitri, V. Canzonieri, F. Visentin, *Polyhedron* **2021**, *207*, 115381.
[23] N. Schulze-Kaysers, M. M. Feuereisen, A. Schieber, *RSC Adv.* **2015**, *5*(89), 73301.
[24] J.-G. Song, C. Cao, J. Li, Y.-J. Xu, Y. Liu, *J. Agric. Food Chem.* **2019**, *67*(14), 4105.
[25] M. Al-Ghorbani, B. Begum, A. Zabiulla, S. V. Mamatha, S. A. Khanum, *J. Chem. Pharm. Res.* **2015**, *7*(5), 281.
[26] M. J. Naim, O. Alam, M. J. Alam, P. Alam, N. Shrivastava, *Int. J. Pharmacol. Pharm. Sci.* **2015**, *3*(1), 40.
[27] R. Kumar, R. V. Srinivasa, S. Kapur, *Int. J. Chem. Sci.* **2016**, *14*, 1777.
[28] F. Arshad, M. F. Khan, W. Akhtar, M. M. Alam, L. M. Nainwal, S. K. Kaushik, M. Akhter, S. Parvez, S. M. Hasan, M. Shaquiquzzaman, *Eur. J. Med. Chem.* **2019**, *167*, 324.
[29] A. P. Kourounakis, D. Xanthopoulos, A. Tzara, *Med. Res. Rev.* **2020**, *40*, 709.
[30] V. A. Pal'chikov, *Russ. J. Org. Chem.* **2013**, *49*(6), 787.
[31] A. Huseynova, R. Kaya, P. Taslimi, V. Farzaliyev, X. Mammadyarova, A. Sujayev, B. Tüzün, U. M. Kocyigit, S. Alwasel, İ. Gulçin, *J. Biomol. Struct. Dyn.* **2022**, *40*(1), 236.
[32] S. Hashmi, S. Khan, Z. Shafiq, P. Taslimi, M. Ishaq, N. Sadeghian, H. S. Karaman, N. Akhtar, M. Islam, A. Asari, H. Mohamad, İ. Gulçin, *Bioorg. Chem.* **2021**, *107*, 104554.
[33] İ. Gulçin, B. Trofimov, R. Kaya, P. Taslimi, L. Sobenina, E. Schmidt, O. Petrova, S. Malysheva, N. Gusarova, V. Farzaliyev, A. Sujayev, S. Alwasel, C. T. Supuran, *Bioorg. Chem.* **2020**, *103*, 104171.
[34] P. Taslimi, K. Turhan, F. Türkan, H. Sedef Karaman, Z. Turgut, İ. Gulcin, *Bioorg. Chem.* **2020**, *97*, 103647.
[35] N. Lolak, S. Akocak, C. Türkeş, P. Taslimi, M. Işık, Ş. Beydemir, İ. Gülçin, M. Durgun, *Bioorg. Chem.* **2020**, *100*, 103897.
[36] G. Bitencourt-Ferreira, de W. F. Azevedo, *Humana*, New York, NY **2019**, p. 149.
[37] S. Kusumaningrum, E. Budianto, S. Kosela, W. Sumaryono, F. Juniarti, *J. Appl. Sci.* **2014**, *4*, 47.
[38] S. Daşgın, Y. Gök, D. Barut Celepci, P. Taslimi, M. İzmirli, A. Aktaş, İ. Gülçin, *J. Mol. Struct.* **2021**, *1228*, 129442.
[39] F. Erdemir, D. B. Celepci, A. Aktaş, Y. Gök, R. Kaya, P. Taslimi, Y. Demir, İ. Gulçin, *Bioorg. Chem.* **2019**, *91*, 103134.
[40] A. Behçet, P. Taslimi, Y. Gök, A. Aktaş, T. Taskin-Tok, İ. Gülçin, *Arch. Pharm.* **2022**, *355*, e2200276.
[41] M. J. Frisch, G. W. Trucks, H. B. Schlegel, G. E. Scuseria, M. A. Robb, J. R. Cheeseman, G. Scalmani, V. Barone, B. Mennucci, G. A. Petersson, *Gaussian 09*, *Revision E.01*, Gaussian, Inc. Wallingford CT **2009**.
[42] F. Kiefer, K. Arnold, M. Kunzli, L. Bordoli, T. Schwede, *Nucleic Acids Res.* **2009**, *37*, D387.
[43] K. Arnold, L. Bordoli, J. Kopp, T. Schwede, *Bioinformatics* **2006**, *22*, 195.
[44] N. Guex, M. C. Peitsch, T. Schwede, *Electrophoresis* **2009**, *30*, S162.
[45] O. Trott, A. J. Olson, *J. Comput. Chem.* **2010**, *31*, 455.
[46] Accelrys Software Inc, *Discovery Studio Modeling Environment*, *Release 3.5*, Accelrys Software Inc, San Diego **2013**.
[47] Rigaku Corporation, *CrysAlis(Pro) Software System; Version 1.171.38.4*, Rigaku Corporation, Oxford, UK **2015**.
[48] G. M. Sheldrick, *Acta Crystallogr. A: Found. Adv.* **2015**, *A71*, 3.
[49] G. M. Sheldrick, *Acta Crystallogr. C Struct. Chem.* **2015**, *C71*, 3.
[50] A. L. Spek, *J. Appl. Crystallogr.* **2003**, *36*, 7.
[51] O. V. Dolomanov, L. J. Bourhis, R. J. Gildea, J. A. K. Howard, H. Puschmann, *J. Appl. Crystallogr.* **2009**, *42*, 339.
[52] A. Aktaş, D. Barut Celepci, R. Kaya, P. Taslimi, Y. Gök, M. Aygün, İ. Gülçin, *Polyhedron.* **2019**, *159*, 345.
[53] J. A. Verpoorte, S. Mehta, J. T. Edsall, *J. Biol. Chem.* **1967**, *242*, 4221.
[54] İ. Timur, U. M. Koçyiğit, T. Dastan, S. Sandal, A. O. Ceribasi, P. Taslimi, İ. Gülçin, M. Koparir, M. Karatepe, M. Ciftci, *J. Biochem. Mol. Toxicol.* **2019**, *33*(1), e22239.
[55] C. Bayrak, P. Taslimi, H. S. Karaman, İ. Gulcin, A. Menzek, *Bioorg. Chem.* **2019**, *85*, 128.
[56] G. L. Ellman, K. D. Courtney, V. Andres, R. M. Featherstone, *Biochem. Pharmacol.* **1961**, *7*, 88.
[57] M. Huseynova, A. Medjidov, P. Taslimi, M. Aliyeva, *Bioorg. Chem.***2019**, *83*, 55.
[58] Y. Tao, Y. Zhang, Y. Cheng, Y. Wang, *Biomed. Chromatogr.* **2013**, *27*(2), 148.
[59] A. R. Pasha, A. Khan, S. Ullah, S. A. Halim, J. Hussain, M. Khalid, M. M. Naseer, A. F. El-kott, S. Negm, A. Al-Harrasi, Z. Shafiq, *Sci. Rep.* **2023**, *13*(1), 1877.
[60] S. A. Patil, S. A. Patil, R. Patil, R. S. Keri, S. Budagumpi, G. R. Balakrishna, M. Tacke, *Future Med. Chem.* **2015**, *7*(10), 1305.
[61] N. Arif, Z. Shafiq, K. Mahmood, M. Rafiq, S. Naz, S. A. Shahzad, U. Farooq, A. H. Bahkali, A. M. Elgorban, M. Yaqub, A. El-Gokha, *ACS omega* **2022**, *7*(32), 28605.
[62] A. Imran, M. T. Shehzad, S. J. A. Shah, M. Laws, T. Al-Adhami, K. M. Rahman, I. A. Khan, Z. Shafiq, J. Iqbal, *ACS omega* **2022**, *7*(30), 26425.
[63] A. Aktaş, G. Yakalı, Y. Demir, İ. Gülçin, M. Aygün, Y. Gök, *Heliyon* **2022**, *8*(9), e10625.
[64] F. Türker, C. Gürses, D. Barut Celepci, A. Aktaş, B. Ateş, Y. Gök, *Arch. Pharm.* **2019**, *352*(12), 1900187.

10990461, 0, Downloaded from https://onlinelibrary.wiley.com/doi/10.1002/jbt.23554 by Dokuz Eylul University, Wiley Online Library on [24/10/2023]. See the Terms and Conditions (https://onlinelibrary.wiley.com/terms-and-conditions) on Wiley Online Library for rules of use; OA articles are governed by the applicable Creative Commons License

[65] J. Sun, G. Wang, *Acta Crystallogr. E Struct. Rep. Online* **2011**, *E67*, m165.
[66] F. E. Hahn, T. Pape, C. Holtgrewe, *Z. fur Naturforsch. B* **2004**, *59*(9), 1051.
[67] Ö. Doğan, N. Gürbüz, İ. Özdemir, B. Çetinkaya, O. Şahin, O. Büyükgüngör, *Dalton Trans.* **2009**, *35*, 7087.
[68] F. H. Allen, O. Kennard, D. G. Watson, L. Brammer, A. G. Orpen, R. Taylor, *J. Chem. Soc. Perkin Trans.* **1987**, *1*, 1.
[69] M. Akkurt, S. Öztürk, N. Şireci, H. Küçükbay, O. Büyükgüngör, *Acta Cryst.* **2004**, *E60*, o1185.
[70] D. Cremer, J. A. Pople, *J. Am. Chem. Soc.* **1975**, *97*, 1354.
[71] C. A. Janiak, *J. Chem. Soc. Dalton.* **2000**, *21*, 3885.
[72] M. Ekiz, A. Tutar, S. Ökten, B. Bütünc, Ü. M. Koçyiğit, P. Taslimi, G. Topçu, *Arch. Pharm.* **2018**, *351*, 1800167.
[73] İ. Gulçin, P. Taslimi, *Expert Opin. Ther. Pat.* **2018**, *28*(7), 541.
[74] P. Taslimi, İ. Gulçin, *J. Food Biochem.* **2018**, *42*(3), e12516.
[75] P. Taslimi, C. Çağlayan, F. Farzaliyev, O. Nabiyev, A. Sujayev, F. Türkan, R. Kaya, İ. Gulçin, *J. Biochem. Mol. Toxicol.* **2018**, *32*(4), e22042.
[76] Q. N. Tariq, S. Malik, A. Khan, M. M. Naseer, S. U. Khan, A. Ashraf, M. Ashraf, M. Rafiq, K. Mahmood, M. N. Tahir, Z. Shafiq, *Bioorg. Chem.***2019**, *84*, 372.
[77] V. G. Klochkov, E. N. Bezsonova, M. Dubar, D. D. Melekhina, V. V. Temnov, E. V. Zaryanova, N. A. Lozinskaya, D. A. Babkov, A. A. Spasov, *Bioorganic Med. Chem. Lett.* **2022**, *55*, 128449.
[78] S. B. Kassa, P. Taslimi, Ş. Özel, B. Gür, İ. Gülçin, Y. Onganer, *Colloids Surf. A Physicochem. Eng. Asp.* **2022**, *632*, 127839.
[79] S. Akocak, P. Taslimi, N. Lolak, M. Işık, M. Durgun, Y. Budak, C. Türkeş, İ. Gülçin, Ş. Beydemir, *Chem. Biodivers.* **2021**, *18*, e2000958.

SUPPORTING INFORMATION

Additional supporting information can be found online in the Supporting Information section at the end of this article.

How to cite this article: A. Behçet, P. Taslimi, B. Şen, T. Taskın-Tok, A. Aktaş, Y. Gök, M. Aygün, İ. Gülçin, *J. Biochem. Mol. Toxicol.* **2023**, e23554. https://doi.org/10.1002/jbt.23554

10990461, 0, Downloaded from https://onlinelibrary.wiley.com/doi/10.1002/jbt.23554 by Dokuz Eylul University, Wiley Online Library on [24/10/2023]. See the Terms and Conditions (https://onlinelibrary.wiley.com/terms-and-conditions) on Wiley Online Library for rules of use; OA articles are governed by the applicable Creative Commons License